Elsevier Editorial System(tm) for Journal of Controlled Release

Manuscript Draft

Manuscript Number: JCR-D-17-00787R1

Title: Increased delivery of chemotherapy to the vitreous by inhibition of the blood-retinal barrier

Article Type: Research paper

Keywords: blood-retinal barrier; retinoblastoma; topotecan; pantoprazole; microdialysis; rabbit; ABC transporters; BCRP; ABCG2/BCRP; P-gp; ABCB1/P-gp; pediatric cancer; vitreous; retina; distribution; delivery; xenograft

Corresponding Author: Dr. Angel M Carcaboso, PhD

Corresponding Author's Institution: Sant Joan de Deu Research Foundation

First Author: Guillem Pascual-Pasto

Order of Authors: Guillem Pascual-Pasto; Nagore G Olaciregui; Javier A Opezzo; Helena Castillo-Ecija; Maria Cuadrado-Vilanova; Sonia Paco; Ezequiel M Rivero; Monica Vila-Ubach; Camilo A Restrepo-Perdomo; Montserrat Torrebadell; Mariona Suñol; Paula Schaiquevich; Jaume Mora; Guillermo F Bramuglia; Guillermo L Chantada; Angel M Carcaboso, PhD

Abstract: Treatment of retinoblastoma -a pediatric cancer of the developing retina- might benefit from strategies to inhibit the blood-retinal barrier (BRB). The potent anticancer agent topotecan is a substrate of efflux transporters BCRP and P-gp, which are expressed at the BRB to restrict vitreous and retinal distribution of xenobiotics. In this work we have studied vitreous and retinal distribution, tumor accumulation and antitumor activity of topotecan, using pantoprazole as inhibitor of BCRP and P-gp. We used rabbit and mouse eyes as BRB models and patient-derived xenografts as retinoblastoma models. To validate the rabbit BRB model we stained BCRP and P-gp in the retinal vessels. Using intravitreous microdialysis we showed that the penetration of the rabbit vitreous by lactone topotecan increased significantly upon concomitant administration of pantoprazole ($P = 0.0285$). Pantoprazole also increased topotecan penetration of the mouse vitreous, measured as the vitreous-to-plasma topotecan concentration ratio at the steady state ($P = 0.0246$). Pantoprazole increased topotecan antitumor efficacy and intracellular penetration in retinoblastoma in vitro, but did not enhance intratumor drug distribution and survival in mice bearing the intraocular human tumor HSJD-RBT-2. Anatomical differences with the clinical setting likely limited our in vivo study, since xenografts were poorly vascularized masses that loaded most of the vitreous compartment.
We conclude that pharmacological modulation of the BRB is feasible, enhances anticancer drug distribution into the vitreous and might have clinical implications in retinoblastoma.

Cover Letter

Angel M. Carcaboso, PhD
Institut de Recerca Sant Joan de Déu
Santa Rosa 39-57, Esplugues de Llobregat, Barcelona 08950, SPAIN
Tel: +34 936009751 | *Email:* amontero@fsjd.org

Stefaan De Smedt, PhD
Journal of Controlled Release, Editor

August 17th, 2017

Dear Dr De Smedt,

Thanks for inviting us to submit a revised version of our manuscript. We appreciate the helpful comments of the reviewers. We agree with most of their assessments, and have gone on to significantly improve our manuscript to address their concerns, by adding new data presented in the text and also in two new figure panels and one new supplemental figure. We feel that this has strengthened our work.

We have built a point-by-point rebuttal letter for the reviewers, addressing each of their comments.

Please do not hesitate to contact me if you have questions about our responses. We appreciate your consideration of our revised manuscript, and look forward to hearing from you.

Sincerely yours,

Angel M. Carcaboso

Response to Referees

We have addressed all the points raised by the Reviewers. Our revised text is in blue font in this response and also in the manuscript. Please find our point-by-point responses below.

Reviewer #1: The manuscript reports investigation of topotecan penetration into the eye, and its modulation by pantoprazole. The authors applied different experimental settings (in vivo experiments in rabbits and mice, retinoblastoma cultures), and used advanced research methods (ocular microdialysis, tumorspheres, etc.). The manuscript presents solid experimental data, is well organized and well written. Overall, it appears that pantoprazole can increase the accumulation of lactone topotecan in the eye, but did not alter the total topotecan concentrations (the sum of the lactone and carboxylate forms) and its anti-tumor efficiency.

We thank the reviewer for the overall positive evaluation of our manuscript.

In my view, the following 2 points of critique should be addressed by the authors.

Reviewer 1, Point 1. The mechanism of pantoprazole effect on topotecan vitreous concentrations.
Pantoprazole concentrations in the vitreous fluid and pH of this fluid were not quantified in the animal studies (in rabbits and in mice). Is it possible that pantoprazole effects were pH-dependent (e.g., due to the changes in the pH of the vitreous fluid, or endosomal pH of the retinoblastoma and/or BRB cells), and not due to the Pgp and BCRP inhibition? Increase in lactone/carboxylate ratio (see Fig, 3B) is consistent with increase pH-dependent conversion from carboxylate to lactone at reduced pH.

What is your estimate of vitreous pantoprazole concentrations in animal studies (3.5 mg/kg IV bolus in rabbits, 50 mg/kg IP in mice)? How these concentrations compare to the IC50 values of pantoprazole on the Pgp and BCRP activity in retinoblastoma and/or BRB cells? Do you expect pH changes in the eye tissues/fluids due to pantoprazole treatment?

Response: The reviewer has brought an important question to our attention because there are two mechanisms described by which pantoprazole could modify drug distribution in cells or tissues: 1) by increasing the pH of cellular endosomes (work from the group of Ian Tannock in Toronto [1]), or 2) by inhibiting efflux drug transporters (work from the group of Jan Schellens in Utrecht [2]). Our original manuscript addressed only the second one. Thus, we have included a few additional experiments to address the first mechanism in the new version of the manuscript.

First, we performed one pharmacokinetic experiment to analyze pantoprazole concentrations in plasma, vitreous and retina of athymic nude mice.

New text in Methods:

"Pantoprazole distribution in mouse tissues. *To quantify pantoprazole concentrations in mouse plasma, vitreous and retina, 9 nude mice were injected i.p. with a 50 mg/kg dose of pantoprazole. Plasma samples were obtained at 0.25, 0.5 and 2 h after the administration. Three animals were sacrificed at each time point to collect vitreous and retinas. Plasma, vitreous and retinas were processed as in topotecan studies and processed with cold methanol for protein precipitation. Pantoprazole was quantified by HPLC upon slight modification of a previously described analytical method [3]. Briefly, processed samples were injected (20 µL) in a SIL-20AC autosampler module (Shimadzu, Kyoto, Japan) coupled to a SPD20A UV/VIS detector (Shimadzu) set at 290 nm. The mobile phase was 10 mM NaH_2PO_4 pH 7.2 buffer and*

acetonitrile (60:40), the column was a Tracer Excel 120 ODSA C18 (150 mm × 4.6 mm, 5 µm; Teknokroma, Barcelona, Spain) and the flow rate was 0.5 mL/min. The calibration curves covered the range 0.025-100 µg/mL in plasma and vitreous and 0.25-1000 µg/g in the retina (R^2 = 0.99)."

New text in Results:

*"Pantoprazole concentration-time curves in mouse plasma, vitreous and retina are shown in **Figure 4C**. Achieved Cmax were 109 ± 23, 8.51 ± 1.74 and 49.4 ± 8.5 µM (mean and SD) in plasma, vitreous and retina, respectively. Pantoprazole concentrations were below the limit of quantification in retina and vitreous at 2 h."*

Results are shown in **Response Figure 1** (New **Figure 4C**):

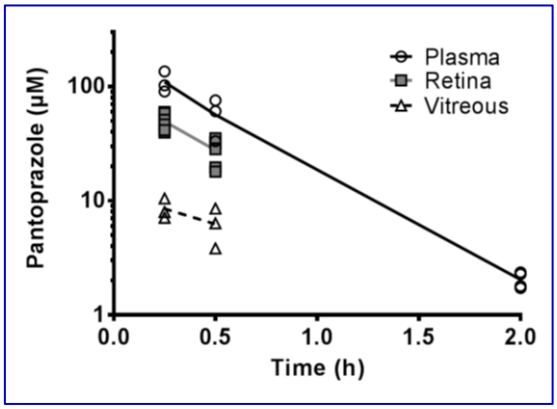

Response Figure 1 (New **Figure 4C**). Pantoprazole concentration-time data in mice after 50 mg/kg pantoprazole i.p.

As the reviewer recalls, topotecan shows pH-dependent conversion from lactone (active) to carboxylate (inactive) at neutral and basic pH. At acidic pH, conversion is reversible from carboxylate to lactone. Thus, hypothetical increments in the vitreous pH due to pantoprazole would have produced a higher proportion of carboxylate in the vitreous. Conversely, a decreased pH value would have favored the lactone form. We addressed this question with two experiments detailed in the Methods. In the first experiment, we measured the pH in the vitreous of mice. In the second experiment, we studied changes in the fluorescence of a pH-sensitive endosomal tracer in retinoblastoma cells. We have added a coauthor, Dr Torrebadell, who performed and analyzed the flow cytometry analysis of retinoblastoma cells.

New text in Methods:

*"**Vitreous pH in pantoprazole-treated mice.** Because the equilibrium of lactone and carboxylate topotecan is reversibly affected by the pH, and pantoprazole is an H^+-ATPase inhibitor that might increase the pH of the target tissues [1], we measured the pH of the vitreous and blood in mice treated with 50 mg/kg pantoprazole. We used a micro-electrode (9810BN, Life Technologies) to measure the pH in small volume samples (up to 1 µL). Four mice were treated either with pantoprazole (n = 2) or with saline (n = 2). After 10 min, they were bled (50 µL) by the tail vein with a heparinized scalpel to measure blood pH. At 0.5 both eyes of each animal were punctured with a 21G needle to collect a vitreous drop (1-2 µL) for pH measurement under ketamine-xylazine anesthesia. The procedure was repeated at 2 h and the mice were sacrificed.*

***Fluorescence of a pH-sensitive tracer in retinoblastoma cells exposed to pantoprazole.** Pantoprazole at concentrations higher than 200 µM increases the endosomal pH of some cancer cell lines in vitro, which can be detected with pH-sensitive markers [1]. Following this approach, we exposed HSJD-RBT-2 cells ($1x10^6$*

cells in 1 mL culture medium) to pantoprazole at concentrations 2.5, 5, 50, 250, 500 and 2000 µM. The pH of the culture medium was measured in each well with a micro-electrode. To study changes in the endosomal pH, after 2 h the pH-sensitive fluorescein 5(6)-isothiocyanate-dextran 10 kDa (FITC-dextran; 500 µg/mL; D1821; Life Technologies) was added to the wells and incubated for 3 h. This endosomal tracer shows higher fluorescence at higher pH values [4]. Cells were then washed with fresh medium, cultured for 2 h and collected by centrifugation. Cell fluorescence was quantified with a flow cytometer (FACSCanto II, BD Biosciences, San Diego, CA)."

Results are shown in **Response Figure 2** (New **Supplemental Figure 3**).

New text in Results:

*"We did not detect significant changes in the physiologic pH of mouse vitreous (mean pH = 7.58; range 7.38-7.78) or blood (mean pH = 7.42; range 7.36-7.47) upon 50 mg/kg pantoprazole treatment (**Supplemental Figure 3A**). In vitro, pH values of culture medium did not change due to the presence of pantoprazole in the range 2.5-2000 µM (**Supplemental Figure 3B**). Fluorescence of HSJD-RBT-2 cells did not change upon incubation with pantoprazole (2.5-500 µM) and FITC-dextran. Cells incubated with 2000 µM pantoprazole (not clinically relevant concentration) showed higher fluorescence signal indicating an increment in the endosomal pH value (**Supplemental Figure 3C**)."*

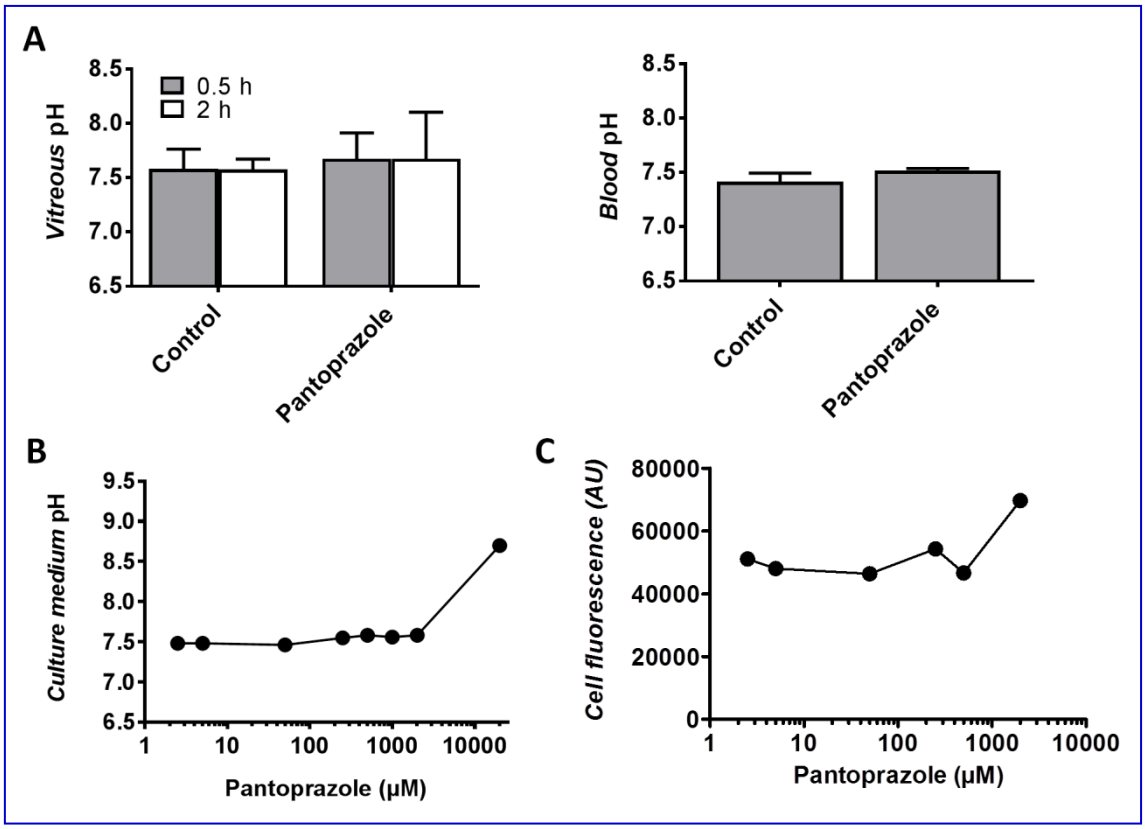

Response Figure 2 (New **Supplemental Figure 3**). Effect of pantoprazole on the pH. A) Vitreous and blood pH in mice receiving i.p injections of pantoprazole 50 mg/kg or saline (mean and SD of 2-4 values). B) pH in the culture medium containing pantoprazole (2-20,000 µM). C) Fluorescence intensity of cells incubated with FITC-dextran was stable in the range 46,000-54,000 arbitrary units (AU) until 500 µM. At 2000 µM the value increased to 70,000 AU, suggesting higher endosomal pH.

New text in Discussion:

"Pantoprazole has been shown to modify drug distribution in tumors by two mechanisms, either by the inhibition of efflux transporters [2] or by induction of changes in the endosomal pH of the tumor cells [1]. Our study supports that the inhibition of the inner BRB was the most likely mechanism by which pantoprazole modified topotecan vitreous distribution in rabbits and mice. In addition, ABC transporters have a higher affinity for lactone topotecan than for the carboxylate counterpart [5]. Thus, our finding of increased lactone (and not carboxylate) exposure in the rabbit vitreous supported further the proposed mechanism of pantoprazole activity through inhibition of the efflux transporters at the BRB. We speculate that topotecan lactone levels achieved in the rabbit vitreous would have reached potentially active concentrations in 3 out of 8 retinoblastoma models (those with IC50 lower than 10 nM; ***Figure 7****) upon co-administration of pantoprazole."*

"To improve our ability to extrapolate these results to the clinical scenario we characterized the pharmacokinetics of pantoprazole in mice. The dosage in the mouse study (50 mg/kg) was limited by the observation of acute toxicity when combined with topotecan at higher pantoprazole dosages. In human patients, a single i.v. dose of 240 mg, combined with doxorubicin, achieves a concentration of 100 µM in plasma [6]. The concentration of pantoprazole in mouse plasma was in a similar range in our study, suggesting that the reported clinical dosage could reach potentially active concentrations at the human BRB. At such systemic exposure (C_{max} 100 µM) in mice, concentrations in the mouse retina (C_{max} 50 µM) inhibited the BRB, leading to increased topotecan exposure in the vitreus. Although we did not test whether this concentration inhibited a BRB model in vitro, previous published work using membrane vesicles from Sf9 cells infected with a baculovirus containing human BCRP showed that pantoprazole reduced 50% of BCRP function at 10 µM and 90% at 50 µM [2]. We did not perform a pharmacokinetic study of pantoprazole in rabbits, although their dosage calculated in mg/kg was in a similar range as compared to the mentioned clinical trial."

To address the question of Reviewer 1 regarding the activity of pantoprazole on P-gp and BCRP activity in retinoblastoma and/or BRB cells, we performed a new experiment to study the range of pantoprazole concentrations that inhibit the efflux pumps at the tumor cell level.

New text in Methods:

"A similar experiment was performed to determine the minimum concentration of pantoprazole able to inhibit efflux transporters in these tumor cells. We exposed tumorspheres to pantoprazole concentrations ranging 5-500 µM and measured intracellular topotecan at 30 min."

Results are shown in **Response Figure 3** (New **Figure 7D)**. We observed that intracellular topotecan in tumor cells increased only at pantoprazole concentrations above 500 µM. This result could help explain why pantoprazole was not efficacious to increase the accumulation and activity of topotecan in the tumor xenograft.

Text in Results:

*[…efflux rate of topotecan from HSJD-RBT-2 tumorspheres was decreased, leading to 23.9 ± 9.4 % higher intracellular topotecan amount after 30 min incubation (****Figure 7C****). Such effect was not significant at pantoprazole concentrations lower than 500 µM (****Figure 7D****).]*

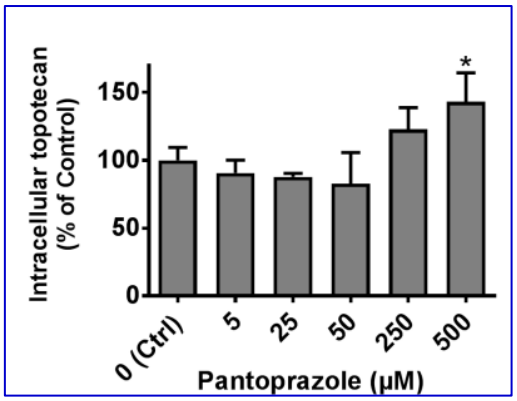

Response Figure 3 (new **Figure 7D**). Concentration-dependent effect of pantoprazole on topotecan accumulation in retinoblastoma HSJD-RBT-2 tumorspheres, in the range 0 (Control; Ctrl) to 500 μM pantoprazole. *P = 0.011; ANOVA.

Thus, with our new experiments we provide evidence supporting that the mechanism of pantoprazole to modify ocular and intracellular distribution of topotecan is not mediated by changes in pH, but most likely by the inhibition of efflux pumps.

Reviewer 1, point 2. The extent of pantoprazole effect on topotecan vitreous concentrations.

The reported "12-fold increase in the penetration of lactone topotecan in the rabbit vitreous" due to pantoprazole treatment (see the abstract and Page 17) is based on the highly heterogeneous experimental data (see Supplemental table, page 20). From 5 rabbits that participated in this experiment, the effect varied from ~4-fold decrease in AUC (in animal 2) to ~500-fold increase (in animal 5). In many samples, lactone topotecan concentrations were below the detection limit (see Fig. 3B), which introduced bias into the calculation of this AUC ratio (e.g., it is not clear how this ratio was calculated for animal 4, which had undetectable lactone topotecan concentrations in all the collected samples).

Please consider to present 'spaghetti' plot of the individual animals' data in Fig. 3B, to describe the inter-animal differences in the pantoprazole effect on topotecan vitreous concentrations, to revise the AUC ratio calculation and its interpretation.

Response: We have reconsidered the analysis and representation of the data upon this important comment. We agree with the reviewer that our previous representation could be misleading given the variability of the data. Consequently we have modified **Figure 3B** to show individual plots (spaghetti plots). The figure (**Response Figure 4**) has improved the previous version now in our view.

Also, we have reconsidered that summarizing the result as “12 fold” increase in lactone topotecan AUC was probably erroneous or at least oversimplified. Thus, we have withdrawn this simplification from the abstract and the main text. Instead, we emphasize now the median AUC value and the range for each group in the text.

Regarding the concern of the reviewer on how we calculated the vitreous-to-plasma AUC ratio of topotecan lactone in animal 4 when not exposed to pantoprazole, we previously calculated it as zero because lactone was not detectable in the vitreous. Upon careful revision of the literature, we noticed that some researchers facing the problem of data below detectable limits prefer to include concentration values of the lowest limit of detection (LLOD) or LLOD/2, instead of zero. We have tested this approach. As a result, the value of the AUC ratio was still very close to zero and our overall analysis and conclusions remained unchanged. Thus, we request to leave the

analysis as performed before (AUC = zero) since it represents well our experimental data in our opinion.

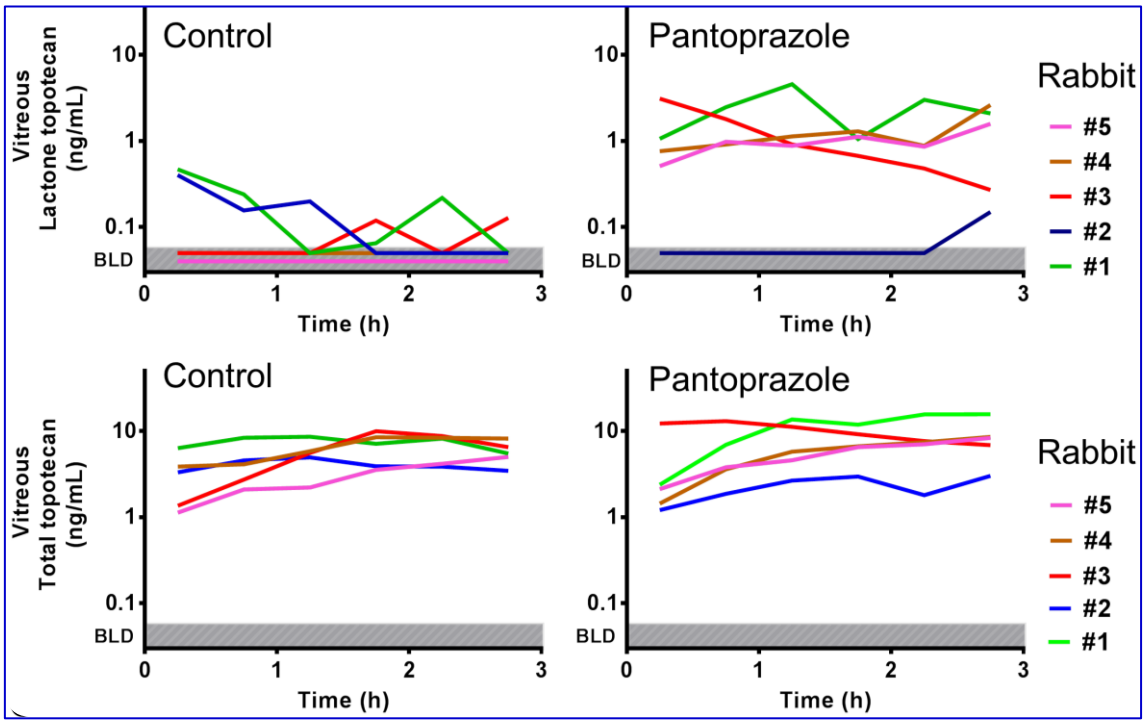

Response Figure 4 (New **Figure 3B**). *Vitreous dialysates concentration-time profiles of unbound topotecan lactone (top panels) or total (bottom panels) in the absence (Control) or presence of pantoprazole treatment (Pantoprazole). Concentration data obtained in 30 min intervals are represented for each of the 5 rabbits, identified with colors, and connected with lines at the median times of each interval. Data represented into the shadowed area are below the limit of detection (BLD).*

New text in Results:

"Median lactone topotecan vitreous-to-plasma AUC ratio (i.e., $P_{vitreous}$), expressed as percentage, was 6.4% (range 0.38-9.4%) after pantoprazole, significantly higher as compared to the topotecan alone treatment ($P_{vitreous}$ = 0.55%; range 0.00-1.6%; P = 0.029; paired t test)."

Reviewer #2: With their manuscript Dr. Pascual-Pasto and colleagues address a relevant topic within the field of ocular delivery, as they report on the evaluation of strategies to inhibit the blood-retinal barrier in order to increase chemotherapy exposure in vitreous and retina. Besides localization studies for specific ABC efflux transporters and substrate anticancer drug distribution studies after BRB inhibition, they also evaluated the antitumor effect of this approach using retinoblastoma xenografts. Despite a negative outcome for the latter, due to limitations of the animal model, the authors performed/reported a very interesting study, in which the topic, the data and the approach are interesting to the journals scientific community. The manuscript certainly contains novel findings that pave the way for future studies. The methodology is sound, the data are nicely presented, accompanied by illustrative figures and thoroughly discussed.

We thank the reviewer for summarizing the relevance of our work.

Nevertheless, the following points need further attention:
Reviewer 2, Point 1. The authors should explain the rationale to use TBP as reference gene in the qRT-PCR experiments. Were more genes tested? State-of-the art RT-PCR

experiments normalize to a set of 3 previously tested genes. What was the reason for only and specifically using the TBP gene?

Response: Following this recommendation we have studied the variability of our previous reference, *TBP*, and analyzed the expression of two alternative genes (*GAPDH* and *ACTB*) as suitable references for the analysis. We concluded that the 3 genes were adequate references given their homogeneous expression and low variability in all the samples. *TBP* presented stable transcription among the retinoblastoma samples (median Ct = 26.82; range 24.93-27.45), as well as *GAPDH* (median Ct = 17.46; range 16.71-18.57) and *ACTB* (median Ct = 22.12; range 21.28-23.84).Thus, we have used the average of the Ct values of the 3 genes as reference for the analysis. We have modified the data in **Supplemental Figure 1** accordingly. We have included a coauthor, Dr Rivero, who helped with this analysis.

Text included in Methods:

"Ct values of reference genes TATA-box binding protein (TBP [7]), glyceraldehyde-3-phosphate dehydrogenase (GAPDH; Hs02786624_g1) and actin beta (ACTB Hs01060665_g1) were averaged to obtain a reference Ct to normalize mRNA expression."

Reviewer 2, Point 2. It would be interesting to also look at expression of the transporters in the retinal pigment epithelium, as a comparison to the data shown for the choroid plexus. Such a (possible) comparison could at minimum be briefly mentioned in the discussion, also in relation to the outer retinal blood barrier.

Response: We have found that the retinal pigment epithelium (RPE) is not positive for BCRP or P-gp staining in the rabbit model, or at least we could not detect it with our method (**Response Figure 5**). This is stated in the text now. At the blood-aqueous barrier, BCRP staining was profusely positive in the basal side of the pigmented epithelium of the ciliary processes (pars plicata). We have included pictures of this interesting finding in the **Response Figure 6**, which is part of the revised **Figure 1**. We have included a coauthor, Dr Restrepo-Perdomo, who helped with the revision of the rabbit tissues.

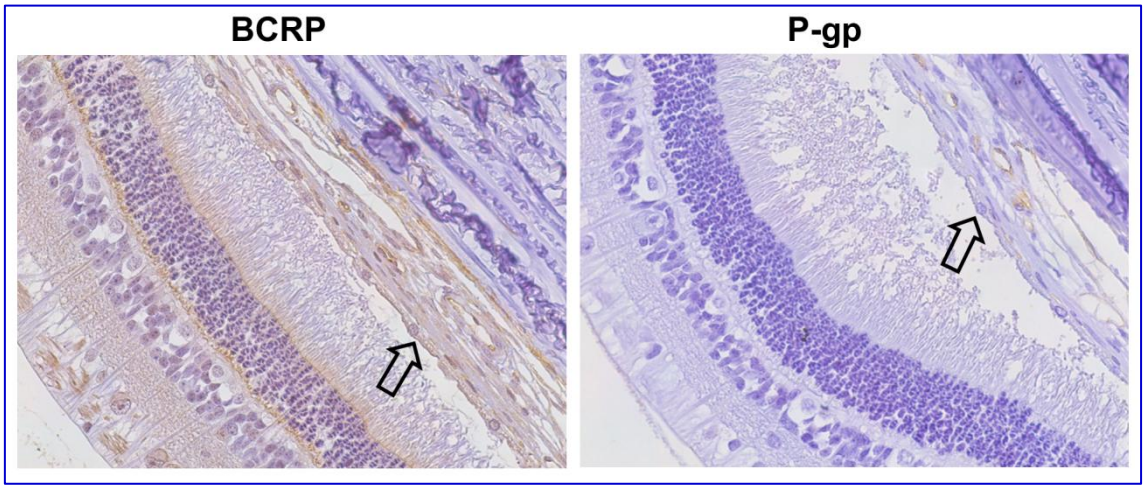

Response Figure 5. BCRP and P-gp are not stained in the RPE (arrows).

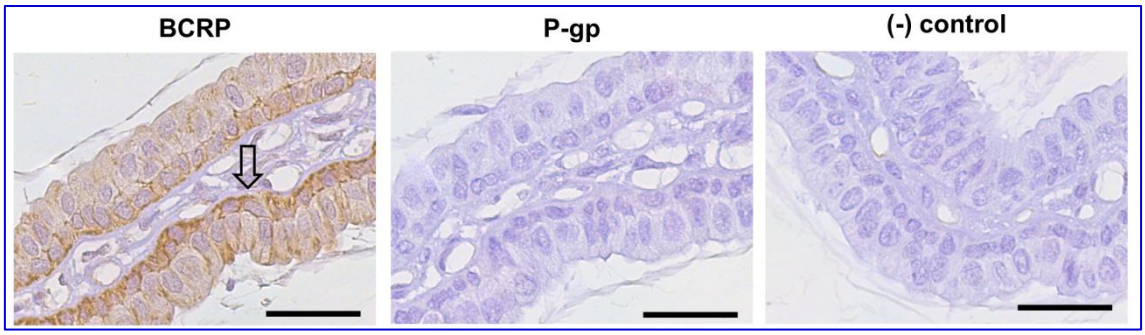

Response Figure 6 (part of New **Figure 1**). BCRP and P-gp staining in the ciliary body.

New text in Results:

"We also found positive BCRP positivity at the pigmented epithelium of the ciliary process (pars plicata), which is part of the blood-aqueous barrier [8]. BCRP and Pgp staining were not apparent in the outer BRB (retinal pigment epithelium)."

Reviewer 2, Point 3. The authors should investigate/report whether the two ABC transporters are expressed at the luminal side of tumor vessels in human eyes and also the localization in tumor cells should preferably be described in a bit more detail.

Response: Our pathologists have confirmed that staining at the vessels is luminal, while tumor cell staining is cytoplasmic. We provide these details in the text in the Results section. This finding was discussed already in the original manuscript (page 29).

New text in Results:

*"Into the retinal tumors of enucleated eyes, tumor vessels (i.e., CD-31-positive vascular structures) were positive for both BCRP and P-gp at the luminal side (**Figure 2**). Positive cytoplasmic BCRP staining was found in tumor cells of 2 of 4 enucleated eyes and P-gp was negative in all tumors cells (**Figure 2**)."*

Reviewer 2, Point 4. It remains puzzling why topotecan lactone distributes more to the vitreous in pantoprazole treated mice, but does not penetrate the retina in these animals. The retina contains retinal vessels and thus BRB inhibition should also result in an increased distribution in the retina. Please comment and discuss the observed difference. Also, is there any reason for the larger SD values in the retina as compared to the vitreous in Figure 4?

Response: The effect of pantoprazole increasing topotecan distribution in the retina was shown in **Figure 4**. However, it was not described as "statistically significant" due to the variability of the results and the limited sample size. To avoid this limitation, we would have needed a larger number of animals.

The larger variability of the results of the retinas, as compared to the one of the vitreous, could have been due to limitations in our technique to dissect these small tissues. Since they remain wet with the ocular fluids upon dissection, it is likely that weights were overestimated in some retinas dissected containing a higher proportion of liquid. In contrast, removing vitreous samples was more reproducible.

Since the main focus of our work was drug distribution into the vitreous, we decided not to include more animals in the studies. We have added text in the discussion to address this comment.

"Because topotecan concentrations in the mouse retinas showed higher variability than the ones in the vitreous, with our sample size we could not confirm whether the effect of pantoprazole to increase drug distribution in the retina was significant, as it was expected according to recently published data [9]. Variability could have been due to

methodological limitations in our technique to dissect and process small tissue samples."

Reviewer 2, Point 5. It is clearly stated that the retina contains more CD31 positive vessels as compared to the vitreal tumor xenografts, but still, the retina nor the tumor show increased topotecan penetration upon pantoprazole treatment. At minimum these issues should be discussed.

Response: We have discussed this further in the text.

*"In vivo, intraocular retinoblastoma xenografts in mice reproduce the main histological features of the original human tumor [7]. Limitations of this model might be related to spatial relation of the tumor and the remaining ocular compartments, since the xenograft grows promptly to load the whole (and limited) volume of the posterior segment of the mouse eye. Also, the vascular count of the orthotopic xenograft was consistent with the previous observation that retinoblastoma cells grow as avascular masses into the mouse eye, impeding the efficacy of systemic chemotherapy [10]. Thus, it is likely that the combination therapy failed to increase topotecan distribution and ocular survival in our study due to the mentioned limitations of the model. In addition, our in vitro studies showed that pantoprazole needs to achieve at least 500 μM to inhibit drug efflux at the tumor cell level (**Figure 7D**). Even in the hypothetical context of an open BRB, it would have been unfeasible to achieve such concentration in our model."*

Reviewer 2, Point 6. Although the manuscript is concisely and well written, the authors may want to consider final language editing by a native English speaker.

Response: Thanks for noting this. We have reviewed carefully the language in the new version of the manuscript.

Reviewer #3: In this paper, the authors have been looking at the effect of the efflux transporters (BCRP and PgP) inhibitor (pantoprazole) over the accumulation of topotecan in the vitreous through reduced efflux on the blood retinal barrier (BRB).
This is an interesting work that shows clearly the presence of the efflux transporters on human eyes and in a rabbit model. As a matter of facts, PK in the vitreous is much in favor of the drug when associated to the inhibitors after IV administration of both in rabbit. The data in vivo in a retinoblastoma model are however disappointing and difficult to explain since PK studies were carried out on healthy animals. They should have been carried out in the xenograft model in mice which I believe is not easy but feasible as described in the literature. I believe these experiments are very important in order to check.

Response: The reviewer considers that our results are clear and requests a pharmacokinetic experiment in animals with tumors. In the previous version of the manuscript we already presented the results of an experiment addressing this specific question (**Figure 5**). Since the reviewer has commented on this point, it is likely that we did not detail or discuss enough the methods and results of such PK experiment in xenografts. Thus, we have reviewed this part of the manuscript to make it more visible for the reader, at all the levels (abstract, methods, results and discussion). Our response to Reviewer 2, Point 5 addressed this point as well. We hope this section is more visible now.

We thank the reviewers for their comments that have allowed us to improve and expand our study.

Sincerely yours,

Angel M. Carcaboso

References

[1] K.J. Patel, C. Lee, Q. Tan, I.F. Tannock, Use of the proton pump inhibitor pantoprazole to modify the distribution and activity of doxorubicin: a potential strategy to improve the therapy of solid tumors, Clin Cancer Res, 19 (2013) 6766-6776.
[2] P. Breedveld, N. Zelcer, D. Pluim, O. Sonmezer, M.M. Tibben, J.H. Beijnen, A.H. Schinkel, O. van Tellingen, P. Borst, J.H. Schellens, Mechanism of the pharmacokinetic interaction between methotrexate and benzimidazoles: potential role for breast cancer resistance protein in clinical drug-drug interactions, Cancer Res, 64 (2004) 5804-5811.
[3] L. Wang, P.J. McNamara, Stereoselective interaction of pantoprazole with ABCG2. I. Drug accumulation in rat milk, Drug Metab Dispos, 40 (2012) 1018-1023.
[4] A. Marchetti, E. Lelong, P. Cosson, A measure of endosomal pH by flow cytometry in Dictyostelium, BMC Research Notes, 2 (2009) 7.
[5] J. Shen, A.M. Carcaboso, K.E. Hubbard, M. Tagen, H.G. Wynn, J.C. Panetta, C.M. Waters, M.A. Elmeliegy, C.F. Stewart, Compartment-specific roles of ATP-binding cassette transporters define differential topotecan distribution in brain parenchyma and cerebrospinal fluid, Cancer Res, 69 (2009) 5885-5892.
[6] I. Brana, A. Ocana, E.X. Chen, A.R. Razak, C. Haines, C. Lee, S. Douglas, L. Wang, L.L. Siu, I.F. Tannock, P.L. Bedard, A phase I trial of pantoprazole in combination with doxorubicin in patients with advanced solid tumors: evaluation of pharmacokinetics of both drugs and tissue penetration of doxorubicin, Invest New Drugs, 32 (2014) 1269-1277.
[7] G. Pascual-Pasto, N.G. Olaciregui, M. Vila-Ubach, S. Paco, C. Monterrubio, E. Rodriguez, U. Winter, M. Batalla-Vilacis, J. Catala, H. Salvador, A. Parareda, P. Schaiquevich, M. Sunol, J. Mora, C. Lavarino, C. de Torres, G.L. Chantada, A.M. Carcaboso, Preclinical platform of retinoblastoma xenografts recapitulating human disease and molecular markers of dissemination, Cancer Lett, 380 (2016) 10-19.
[8] J. Lee, R.M. Pelis, Drug Transport by the Blood-Aqueous Humor Barrier of the Eye, Drug Metab Dispos, 44 (2016) 1675-1681.
[9] M. Bauer, R. Karch, N. Tournier, S. Cisternino, W. Wadsak, M. Hacker, P. Marhofer, M. Zeitlinger, O. Langer, Assessment of P-Glycoprotein Transport Activity at the Human Blood-Retina Barrier with (R)-11C-Verapamil PET, J Nucl Med, 58 (2017) 678-681.
[10] L. White, C.J. Gomer, D.R. Doiron, B.C. Szirth, Ineffective photodynamic therapy (PDT) in a poorly vascularized xenograft model, Br J Cancer, 57 (1988) 455-458.

*Graphical Abstract

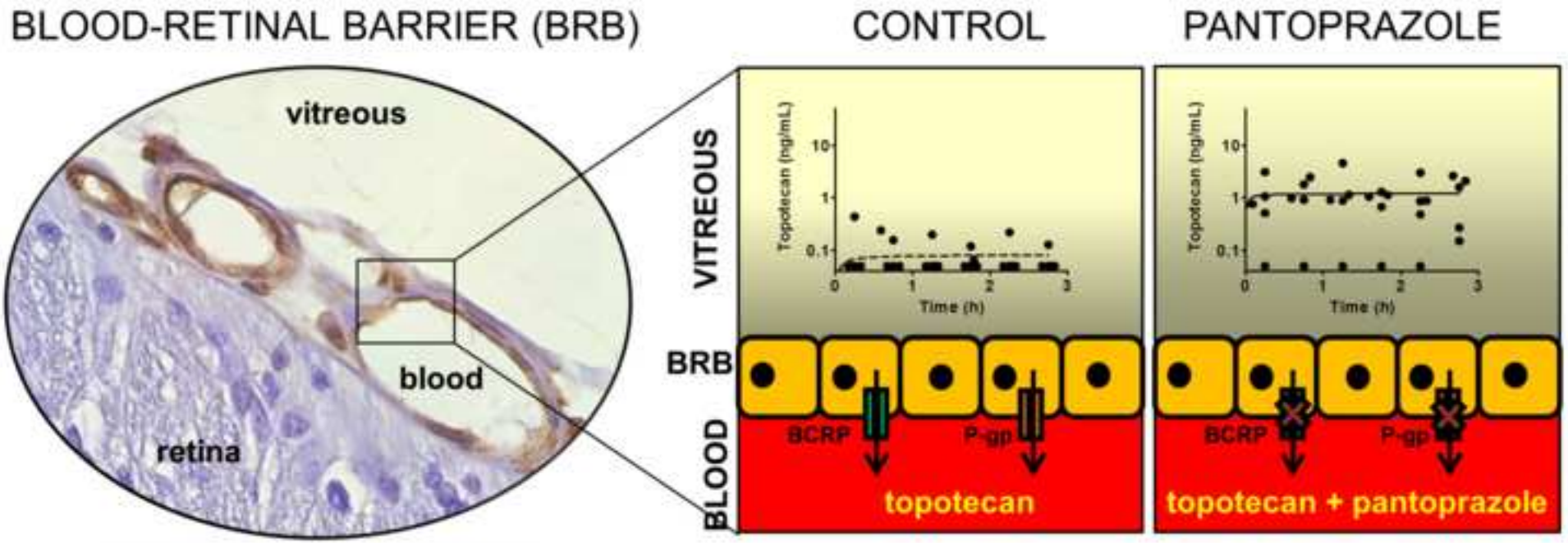

*Revised Manuscript - include embeded figures/tables and also seperate figures/tables
Click here to view linked References

Increased delivery of chemotherapy to the vitreous by inhibition of the blood-retinal barrier

Guillem Pascual-Pasto[a,b], Nagore G. Olaciregui[a,b], Javier A.W. Opezzo[c], Helena Castillo-Ecija[a,b], Maria Cuadrado-Vilanova[a,b], Sonia Paco[a,b], Ezequiel M. Rivero[d], Monica Vila-Ubach[a,b], Camilo A. Restrepo-Perdomo[e], Montserrat Torrebadell[a,b], Mariona Suñol[e], Paula Schaquevich[f,g], Jaume Mora[a,b], Guillermo F. Bramuglia[c], Guillermo L. Chantada[a,b,g,h], Angel M. Carcaboso[a,b*]

[a]*Institut de Recerca Sant Joan de Deu, Barcelona, Spain*

[b]*Department of Pediatric Hematology and Oncology, Hospital Sant Joan de Deu, Barcelona, Spain*

[c]*Department of Pharmacology, Facultad de Farmacia y Bioquimica, Universidad de Buenos Aires, Buenos Aires, Argentina*

[d]*Instituto de Biología y Medicina Experimental, Buenos Aires, Argentina*

[e]*Department of Pathology, Hospital Sant Joan de Deu, Barcelona, Spain*

[f]*Clinical Pharmacokinetics Unit, Hospital de Pediatria JP Garrahan, Buenos Aires, Argentina*

[g]*CONICET, Buenos Aires, Argentina*

[h]*Hospital de Pediatria JP Garrahan, Buenos Aires, Argentina*

*Correspondence: Email: amontero@fsjd.org (A.M. Carcaboso); Tel: +34 936009751 EXT 4420; Fax: +34 936009771

Number of figures: 7; Number of supplemental figures: 3; Number of supplemental tables: 1

Abstract

Treatment of retinoblastoma -a pediatric cancer of the developing retina- might benefit from strategies to inhibit the blood-retinal barrier (BRB). The potent anticancer agent topotecan is a substrate of efflux transporters BCRP and P-gp, which are expressed at the BRB to restrict vitreous and retinal distribution of xenobiotics. In this work we have studied vitreous and retinal distribution, tumor accumulation and antitumor activity of topotecan, using pantoprazole as inhibitor of BCRP and P-gp. We used rabbit and mouse eyes as BRB models and patient-derived xenografts as retinoblastoma models. To validate the rabbit BRB model we stained BCRP and P-gp in the retinal vessels. Using intravitreous microdialysis we showed that the penetration of the rabbit vitreous by lactone topotecan increased significantly upon concomitant administration of pantoprazole ($P = 0.0285$). Pantoprazole also increased topotecan penetration of the mouse vitreous, measured as the vitreous-to-plasma topotecan concentration ratio at the steady state ($P = 0.0246$). Pantoprazole increased topotecan antitumor efficacy and intracellular penetration in retinoblastoma *in vitro*, but did not enhance intratumor drug distribution and survival in mice bearing the intraocular human tumor HSJD-RBT-2. Anatomical differences with the clinical setting likely limited our *in vivo* study, since xenografts were poorly vascularized masses that loaded most of the vitreous compartment.

We conclude that pharmacological modulation of the BRB is feasible, enhances anticancer drug distribution into the vitreous and might have clinical implications in retinoblastoma.

Chemical compounds included in this manuscript: Topotecan (PubChem CID: 60700); Pantoprazole sodium (PubChem CID: 15008962).

Keywords:

blood-retinal barrier; retinoblastoma; topotecan; pantoprazole; microdialysis; rabbit; ABC transporters; BCRP; ABCG2/BCRP; P-gp; ABCB1/P-gp; pediatric cancer; vitreous; retina; distribution; delivery; xenograft

Introduction

Retinoblastoma is the most frequent ocular cancer in children [1]. Patients with advanced intraocular retinoblastoma typically present with massive retinal tumors, frequently disseminated as diffuse small tumors (seeding) in subretinal or vitreous location [2, 3]. Treatment of free-floating vitreous seeding with systemic and intra-arterial chemotherapy remains an unmet medical need because the activity of the inner blood-retinal barrier (BRB) restricts the penetration of xenobiotic agents to the avascular vitreous compartment [4-6]. Recently, drug delivery to the vitreous has been improved by new local techniques of administration, including intravitreal injection, which is now used as standard of care for retinoblastoma vitreous seeding in several ocular oncology centers [7, 8]. However, intravitreal injection is not sufficiently efficient in cases with concomitant presence of active subretinal tumors, and it is technically not feasible when diffuse seeding among the four quadrants of the eye compromise the safety of the procedure [9]. These patients might benefit from new strategies to inhibit the BRB during intravenous or intra-arterial administration of chemotherapy.

Although the function of the BRB is still poorly understood, it may involve the activity of drug transporters located at the retinal vessels such as the ATP-binding cassete (ABC) family (e.g, BCRP/ABCG2, P-gp/ABCB1 and MRPs/ABCCs) [5, 10, 11] and the solute carrier (SLC) family [12, 13]. The question whether the inhibition of these drug transporters at the BRB increases vitreous and retinal distribution of substrate anticancer agents has not been adequately addressed.

Among the clinically relevant anticancer drugs in retinoblastoma, topotecan is a semisynthetic camptothecin showing potent preclinical activity against several pediatric solid tumors [14-16]. Topotecan is given as intravenous low pH formulation to stabilize the active lactone form [17]. In the body fluids, due to neutral pH, the lactone is reversibly hydrolyzed to carboxylate topotecan (inactive), following a first order kinetic process, until reaching the equilibrium at a lactone:carboxylate ratio of approximately 1:9 [18]. The maximum concentration of lactone topotecan achieved in vitreous samples (aspirated with needle) upon the administration of high dose (0.5 mg/kg) in rabbits is 10 ng/mL (20 nM), and the vitreous-to-plasma area under the concentration-time curve (*AUC*) ratio is 0.2, suggesting active efflux from the vitreous compartment [19]. In fact, lactone topotecan is a substrate of the efflux pumps BCRP and P-gp, and inhibition of such pumps at the blood-brain barrier (BBB) leads to increased topotecan penetration of the central nervous system [20]. Because BCRP and P-gp are also located in the inner BRB (retinal vessels) [5, 10], we hypothesized that their inhibition with pantoprazole (a clinically available drug used to reduce acid production of the stomach) could increase topotecan distribution in the vitreous compartment. In combination with chemotherapy agents, pantoprazole inhibits BCRP and P-gp [21, 22]. Pantoprazole has also been shown to enhance the distribution of anticancer agents in solid tumors [23] and it has proven safe at high dose (240 mg; intravenous, i.v.) in adult patients with cancer [24].

In this work we used rabbits and mice as *in vivo* BRB models to study the ocular distribution of topotecan upon coadministration of pantoprazole. We additionally

studied the effect of pantoprazole on topotecan tumor distribution and efficacy in retinoblastoma cells and intraocular xenografts in mice.

Materials and methods

Drugs and reagents. Topotecan (4 mg vials for i.v. injection) was from GSK (Brentford, Middlesex, UK). Pantoprazole sodium was from Baliarda (Buenos Aires, Argentina) or from Sigma-Aldrich (Tres Cantos, Madrid, Spain). Reagents for HPLC were from Merck (Darmstadt, Germany). Reagents for cultures were from Life Technologies (Grand Island, NY, USA).

Immunohistochemistry (IHC). Four micron sections of formalin-fixed, paraffin-embedded (FFPE) tissues were used. Human enucleated eyes with retinoblastoma were obtained under an IRB-approved protocol and informed consent. Primary antibodies anti-BCRP/ABCG2 (clone BXP-21, ab3380; 1:50; Abcam, Cambridge, UK), anti-P-glycoprotein (EPR10363, ab170903; 1:250; Abcam), anti-CD31 (ab28364; 1:100; Abcam) and anti-human nuclei (MAB4383, 1:200; Merck Millipore, Watford, UK) were used to stain BCRP (rabbit and human), P-gp (rabbit and human), endothelial cells (mouse and human), and human nuclei, respectively.

Vitreous and plasma protein binding in rabbits. The unbound fraction of drugs determines the distribution processes through the active transport mechanisms involved in the BBB, the BRB and the tumor cells [25]. Thus, we calculated the unbound fraction of lactone and carboxylate topotecan in vitreous and plasma. We used the ultrafiltration method (Centrifree Ultrafiltration Device with Ultracel YM-T membrane, Merck Millipore, Billerica, MA). Briefly, topotecan

at clinically relevant concentrations 20 and 100 ng/mL (50:50 mixture of carboxylate and lactone forms) was incubated 10 min in rabbit vitreous and plasma, respectively, at 37 ºC, and then ultrafiltrated in triplicate. Vitreous and plasma protein binding were calculated as previously described [26].

Effect of pantoprazole on topotecan distribution in rabbit vitreous dialysates. A previously described ocular microdialysis sampling method was used to study the concentrations of free (protein-unbound) lactone and carboxylate topotecan in the vitreous of New Zealand albino rabbit eyes [27]. This animal experiment was approved by the local animal experimentation committee (CICUAL 5947817). Each animal (5 rabbits, 10 eyes; purchased from Izaguirre, Buenos Aires, Argentina) received both treatments, i.e., topotecan 0.25 mg/kg i.v. bolus, or topotecan 0.25 mg/kg i.v. bolus preceded by pantoprazole 3.5 mg/kg bolus, 15 min before topotecan. Treatments were separated by 7 days and assigned randomly the first day. The first day of the experiments a central catheter was placed in the right jugular vein of each rabbit to infuse intravenous drugs and to withdraw blood samples under general anesthesia with ketamine-xylazine (37.5 mg/kg and 5 mg/kg). An intravitreal microdialysis probe was sutured to the sclera of the right eye and vitreous dialysates were obtained under general anesthesia [27]. After a 40 min period of equilibration of the probe, the animal received the treatments i.v., vitreous dialysates were obtained every 30 min for 3 h and both topotecan forms (lactone and carboxylate) were quantified immediately by HPLC as previously described [19]. A retrodialysis experiment infusing 500 ng/mL topotecan was performed at the end of the experiment to calibrate the probe, and the animals were recovered [27]. Upon profuse rinsing of the central catheter, blood

samples were obtained at 0.05, 0.25, 1.5 and 3 h after the administration of topotecan, plasma was precipitated in cold methanol and supernatants were analyzed immediately by HPLC [19]. Seven days later (day 8) a similar experiment was performed by cannulating the left jugular vein and inserting a microdialysis probe in the left eye before the administration of the second treatment. Thus, after the completion of both experiments, each animal produced paired vitreous and plasma topotecan pharmacokinetic data with and without pantoprazole. Vitreous dialysate and plasma samples were obtained at time zero during the second experiment, to ensure complete wash out of topotecan received in the previous (day 1) experiment. After the end of the second microdialysis experiment animals were euthanized under general anesthesia with a rapid intravenous bolus injection of sodium thiopental (100 mg).

Topotecan *AUC*s were calculated by the trapezoid method to quantify exposure to unbound topotecan (lactone and total) in plasma ($AUC_{u,plasma}$) and vitreous ($AUC_{u,vitreous}$) of each individual experiment. The maximum concentration achieved in plasma (C_{max}) was calculated by extrapolation at time 0 of the initial fast exponential decay curve. The extent of penetration of vitreous by unbound topotecan ($P_{vitreous}$) was calculated as the vitreous-to-plasma *AUC* ratio (Equation 1).

$$P_{vitreous} = \frac{AUC_{u,vitreous}}{AUC_{u,plasma}} \quad (1).$$

Retinoblastoma cultures and xenografts. Seven patient-derived retinoblastoma tumor models (HSJD-RBT-1, HSJD-RBVS-1, HSJD-RBT-2, HSJD-RBVS-3, HSJD-RBT-5, HSJD-RBT-7 and HSJD-RBT-8) were cultured as

tumorspheres in neural stem cell medium (serum-free) [28]. Retinoblastoma cell line Y79 was obtained from Sigma-Aldrich and cultured as previously described [28]. Intraocular xenografts were established in immunodeficient mice (athymic nude; 6 week old; Envigo, Barcelona, Spain) under the approved animal protocol number 542/15, as already described [28].

Expression of BCRP and P-gp in retinoblastoma cultures and xenografts. The expression of efflux transporters BCRP and P-gp at the tumor cell level alters the intracellular distribution and activity of topotecan [29]. Thus, we examined the expression of mRNA of both genes in the patient-derived retinoblastoma models. Total RNA from cultured cells or xenografts was isolated and processed by real-time quantitative RT-PCR (qRT-PCR) as previously described [28]. We used fluorescent probes (Taqman Gene Expression Assays, Applied Biosystems, Rotkreuz, Switzerland) for *ABCG2/BCRP* (Hs01053790_m1) and *ABCB1/P-gp* (Hs00184500_m1). Ct values of reference genes TATA-box binding protein (*TBP* [28]), glyceraldehyde-3-phosphate dehydrogenase *(GAPDH*; Hs02786624_g1) and actin beta (*ACTB* Hs01060665_g1) were averaged to obtain a reference Ct to normalize mRNA expression.

Effect of pantoprazole on topotecan penetration of mouse vitreous, retina and orthotopic retinoblastoma xenografts at the steady state. Topotecan-loaded osmotic devices (Alzet 2001D) pumping the drug at a continuous rate of 7 µg/h were implanted subcutaneously (s.c.) in athymic nude mice as previously described [29]. The extent of penetration of tissue (P_{tissue}) by lactone and total topotecan was calculated as the tissue (vitreous, retina or tumor)-to-plasma

concentration ratio at the steady state (i.e., at constant plasma concentration) [26] (Equation 2):

$$P_{tissue} = \frac{C_{ss,tissue}}{C_{ss,plasma}} \quad (2),$$

where $C_{ss,tissue}$ is the steady state concentration in tissue (vitreous, retina or tumor) and $C_{ss,plasma}$ is the steady state concentration in plasma.

To calculate topotecan penetration of vitreous and retina ($P_{vitreous}$ and P_{retina}) in the presence and absence of pantoprazole, osmotic pumps were implanted in 12 mice without tumors. After 5 h of continuous infusion (at the steady state), 6 mice received an intraperitoneal (i.p.) dose of pantoprazole 50 mg/kg, and the remaining 6 received the same volume of saline. 2 h after the administration of pantoprazole or saline, mice were anesthetized with ketamine-xylazine (100-10 mg/kg), bled by cardiac puncture and sacrificed to collect vitreous and retinas. Plasma and vitreous were mixed (1:4) with cold methanol and retinas were snap-frozen. All samples were stored at -80 ºC until processed for analysis [19].

To study the effect of pantoprazole on the distribution of topotecan in intraocular retinoblastoma xenografts, HSJD-RBT-2 cells were injected orthotopically in both eyes of 7 nude mice [28]. Tumor growth was monitored by visual inspection until evidence of tumor in the anterior chamber (at that point, the posterior chamber is 100% loaded with tumor [28]). Then, topotecan-loaded pumps were implanted as described in the previous experiment, pantoprazole or saline was administered to mice 5 h after infusion, and samples (blood and intraocular tumors) were collected 2 h later, processed and stored at -80 ºC until analysis.

Pantoprazole distribution in mouse tissues. To quantify pantoprazole concentrations in mouse plasma, vitreous and retina, 9 nude mice were injected i.p. with a 50 mg/kg dose of pantoprazole. Plasma samples were obtained at 0.25, 0.5 and 2 h after the administration. Three animals were sacrificed at each time point to collect vitreous and retinas. Plasma, vitreous and retinas were processed as in topotecan studies and processed with cold methanol for protein precipitation. Pantoprazole was quantified by HPLC upon slight modification of a previously described analytical method [30]. Briefly, processed samples were injected (20 µL) in a SIL-20AC autosampler module (Shimadzu, Kyoto, Japan) coupled to a SPD20A UV/VIS detector (Shimadzu) set at 290 nm. The mobile phase was 10 mM NaH_2PO_4 pH 7.2 buffer and acetonitrile (60:40), the column was a Tracer Excel 120 ODSA C18 (150 mm × 4.6 mm, 5 µm; Teknokroma, Barcelona, Spain) and the flow rate was 0.5 mL/min. The calibration curves covered the range 0.025-100 µg/mL in plasma and vitreous and 0.25-1000 µg/g in the retina (R^2 = 0.99).

Vitreous pH in pantoprazole-treated mice. Because the equilibrium of lactone and carboxylate topotecan is reversibly affected by the pH, and pantoprazole is an H^+-ATPase inhibitor that might increase the pH of the target tissues [23], we measured the pH of the vitreous and blood in mice treated with 50 mg/kg pantoprazole. We used a micro-electrode (9810BN, Life Technologies) to measure the pH in small volume samples (up to 1 µL). Four mice were treated either with pantoprazole (n = 2) or with saline (n = 2). After 10 min, they were bled (50 µL) by the tail vein with a heparinized scalpel to measure blood pH. At 0.5 both eyes of each animal were punctured with a 21G needle to collect a

vitreous drop (1-2 µL) for pH measurement under ketamine-xylazine anesthesia. The procedure was repeated at 2 h and the mice were sacrificed.

Fluorescence of a pH-sensitive tracer in retinoblastoma cells exposed to pantoprazole. Pantoprazole at concentrations higher than 200 µM increases the endosomal pH of some cancer cell lines *in vitro*, which can be detected with pH-sensitive markers [23]. Following this approach, we exposed HSJD-RBT-2 cells ($1x10^6$ cells in 1 mL culture medium) to pantoprazole at concentrations 2.5, 5, 50, 250, 500 and 2000 µM. The pH of the culture medium was measured in each well with a micro-electrode. To study changes in the endosomal pH, after 2 h the pH-sensitive fluorescein 5(6)-isothiocyanate-dextran 10 kDa (FITC-dextran; 500 µg/mL; D1821; Life Technologies) was added to the wells and incubated for 3 h. This endosomal tracer shows higher fluorescence at higher pH values [31]. Cells were then washed with fresh medium, cultured for 2 h and collected by centrifugation. Cell fluorescence was quantified with a flow cytometer (FACSCanto II, BD Biosciences, San Diego, CA).

***In vivo* efficacy in retinoblastoma-bearing mice.** HSJD-RBT-2 cells were injected bilaterally in the posterior ocular chambers of 20 nude mice. Seven days after tumor inoculation mice were randomized in 4 groups. The group *Topotecan* was treated with 2 cycles of topotecan 0.6 mg/kg, administered i.p. in days 1 to 5 of the week (5 days-on-2-off schedule) for 2 consecutive weeks. The second cycle started at day 21. The group *Pantoprazole* was treated with pantoprazole 50 mg/kg administered i.p. in the same schedule as the *Topotecan* group. The group *Combination* was treated with topotecan and pantoprazole treatments as in the first two groups. Pantoprazole injections were administered 0.5 h before topotecan. The group *Control* received saline

injections i.p. Ocular survival was the time (days) to develop intraocular tumors invading the posterior and anterior chambers of the ocular globes causing proptosis [28].

Drug activity assays. Topotecan antiproliferative activity is well known in retinoblastoma cell lines, but only partially in the new patient-derived serum-free cultures [32]. Thus, 5,000 cells of each retinoblastoma model were cultured in 96-well plates (Costar, Cambridge, MA) and incubated at 37 ºC for 24 h. Then, topotecan (0.0004-15 µM) was added to the cultures (6 wells per concentration). The MTS assay (Promega, Fitchburg, WI, USA) was used after 72 h to determine the percentage of viable cells after each treatment as compared to control wells that were considered 100 % viable. The half maximal inhibitory concentration (IC50), defined as the concentration of drug required to cause a reduction of 50 % in cell viability, was calculated with Graphpad Prism 5 software (La Jolla, CA).

Topotecan antitumor activity can be increased *in vitro* by pharmacological inhibition of BCRP and P-gp [33, 34]. Thus, we incubated HSJD-RBT-2 cells (10,000 cells per well in 96-well round-bottom plates; 6 wells per experimental condition) with pantoprazole (500 µM) for 2 h in a final volume of 150 µL. Then, medium containing topotecan (50 µL) was added to the wells to achieve topotecan concentrations of 2 nM, 20 nM and 200 nM (values of IC10, IC50 and IC90 respectively). After 30 min incubation, the plates were centrifuged gently (3 min at 300 g) and the drug-containing medium was aspirated and replaced with fresh medium. Cell viability was determined 72 h later by the MTS assay.

Accumulation of topotecan in retinoblastoma tumorspheres. We studied whether topotecan accumulation in HSJD-RBT-2 cells increased upon exposure to pantoprazole. Retinoblastoma tumorspheres were dissagregated and cultured ($1x10^6$ cells in 3 mL medium) in 6-well plates until the new tumorspheres achieved a diameter of at least 300 µm. Then, 1 mL of medium with or without pantoprazole was added (final concentration, 500 µM). After 2 h incubation, 2 mL of medium containing topotecan was added (final concentration 10 µM, i.e., 4.6 µg/mL). After 1, 5, 15 and 30 min incubation at 37 ºC the medium was rapidly aspirated, tumorspheres were collected in 15 mL tubes and washed with ice-cold PBS (2 x 5 mL). Finally, 20 µL of ice-cold water was aggregated on top of the cell pellets to lyse the cells, and the lysates were transferred to microcentrifuge tubes on ice. Samples were mixed vigorously with 80 µL of cold methanol and centrifuged for 10 min at 12,000 rpm. The supernatants were stored at −80°C until HPLC assay [19]. A similar experiment was performed to determine the minimum concentration of pantoprazole able to inhibit efflux transporters in these tumor cells. We exposed tumorspheres to pantoprazole concentrations ranging 5-500 µM and measured intracellular topotecan at 30 min.

Statistics. Statistical analysis was performed with Graphpad Prism 5 software (La Jolla, CA). Topotecan pharmacokinetic variables in individual rabbits with and without pantoprazole were compared with paired *t* tests. Unpaired data were compared with Student's *t* test or ANOVA. Median eye survival in retinoblastoma xenografts was calculated with Kaplan-Meyer curves and the log-rank test with Bonferroni-corrected threshold was used to compare survival

curves between treatments. Aggregate data are presented as mean values with standard deviation.

Results

Expression of topotecan transporters in the rabbit BRB and in enucleated human eyes with retinoblastoma. Topotecan transporters BCRP and P-gp are expressed in the mouse and human retinal vasculature [5, 10, 13], but the rabbit model, to our knowledge, remains not characterized. Thus, our first goal was to confirm the presence of these transporters in the rabbit BRB model. As expected for the rabbit eye anatomy, the retinal vasculature was limited to axial vessels in a horizontal plane radiating from the optic nerve, consistent with a merangiotic pattern [35]. BCRP and P-gp expression was positive in the luminal side of the endothelial cells of the retinal vessels (**Figure 1**).

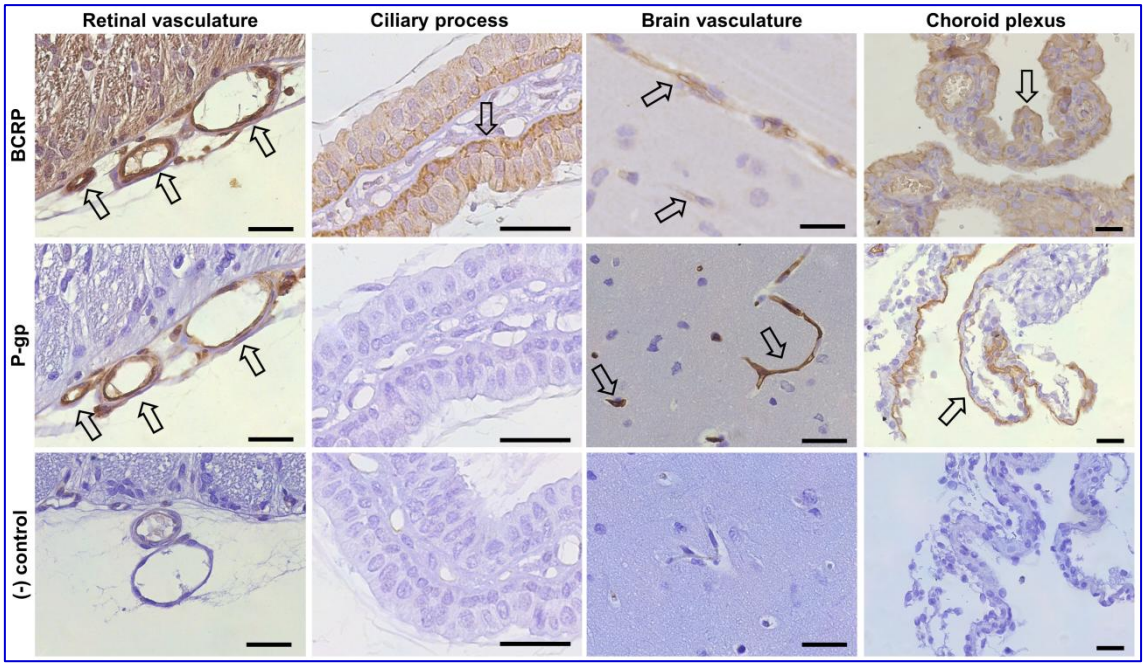

Figure 1. Expression of BCRP and P-gp in the rabbit. The merangiotic retinal vessels were positive for BCRP and P-gp staining (arrows) in the luminal side. BCRP was

positive in the pigmented epithelium of the ciliary process, in the side facing the choroidal blood supply. In the rabbit brain, BCRP and P-gp staining were positive in the apical side of the choroid plexus ependymal cells and in the luminal side of the BBB capillaries. Negative controls (tissue slides incubated with no primary antibody) are shown for comparison. Pictures were obtained using a microscope with a 40x objective. Bars are 25 µm.

To confirm the specificity of the antibodies for BCRP and P-gp, we sought to detect positive staining at the BBB (brain vessels) and the choroid plexus. Consistently with published data in mice and rats [36, 37], BCRP and P-gp staining in rabbits was positive in the luminal side of brain vessels and in the apical side of the choroid plexus (**Figure 1**). We also found positive BCRP at the pigmented epithelium of the ciliary process (pars plicata), which is part of the blood-aqueous barrier [38]. BCRP and Pgp staining were not detectable in the outer BRB (retinal pigment epithelium).

Next, we studied topotecan transporters in human eyes of four patients enucleated due to refractory or advanced retinoblastoma. Details of these patients and the cell lines that were established from their tumors have been published elsewhere [28]. Into the retinal tumors of enucleated eyes, tumor vessels (i.e., CD-31-positive vascular structures) were positive for both BCRP and P-gp at the luminal side (**Figure 2**). Positive cytoplasmic BCRP staining was found in tumor cells in 2 of 4 enucleated eyes. P-gp was negative in all tumors cells (**Figure 2**).

BCRP and P-gp mRNA expression was quantified in retinoblastoma cell cultures and HSJD-RBT-2 retinoblastoma xenografts by RT-qPCR. *ABCG2/BCRP* expression was low or negative in tumor cells in culture and in derived xenografts, while *ABCB1/P-gp* was expressed by all the samples

(**Supplemental Figure 1**). HSJD-RBT-2 xenografts expressed 17-fold more *ABCB1/P-gp* than the same cells in culture.

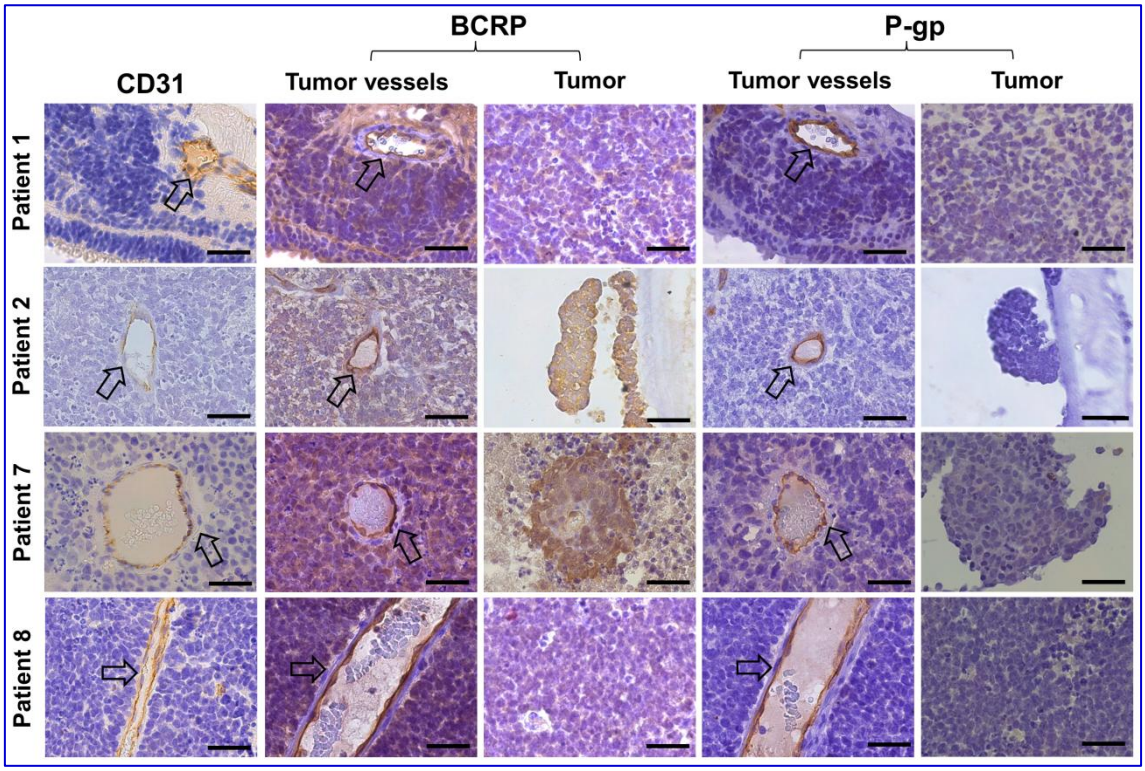

Figure 2. Expression of BCRP and P-gp in human retinoblastoma specimens. Enucleated eyes (4 patients) were fixed in formalin and embedded in paraffin. CD31, BCRP and P-gp were stained in tumor areas. Positive staining of tumor vessels is indicated with arrows. Pictures were obtained using a microscope with a 40x objective. Bars are 50 µm.

A few preserved retinal fragments were found into the enucleated eye specimens. In such retinal areas, CD-31-positive retinal vasculature was P-gp-positive and BCRP-negative (**Supplemental Figure 2**). Retinal BCRP staining was extra-vascular, in the nerve fiber layers, consistent with published data [13].

Binding of topotecan to rabbit vitreous and plasma proteins. The protein-unbound fraction of topotecan lactone and carboxylate was 80.9 ± 3.0 % and

93.4 ± 1.7 %, respectively, in vitreous, and 58.8 ± 2.2 % and 91.2 ± 1.2 %, respectively, in plasma.

Effect of pantoprazole on topotecan plasma and vitreous distribution in rabbits. Five rabbits received both treatments (topotecan alone and topotecan preceded by pantoprazole) separated by 7 days. Topotecan concentration-time curves in plasma were not significantly altered by the administration of pantoprazole (**Figure 3A**). Calculated unbound lactone topotecan C_{max} values were 60 ± 17 and 112 ± 54 ng/mL for topotecan alone and topotecan with pantoprazole treatments, respectively (P = 0.168; paired *t* test). Unbound total (lactone + carboxylate) topotecan C_{max} values were 156 ± 27 and 241 ± 121 ng/mL, respectively (P = 0.245; paired *t* test) (**Figure 3A**).

Microdialysis sampling coupled to HPLC analysis provided concentration-time profiles of unbound drug levels in the vitreous compartment. Unbound lactone topotecan concentrations in vitreous dialysates of animals treated with topotecan alone were below the limit of detection in most samples of 3 out of 5 rabbits and they became significantly increased upon the administration of pantoprazole (**Figure 3B**; P = 0.0001 upon time-matched and animal-matched concentration data comparison; paired *t* test). Unbound total topotecan levels were slightly higher after pantoprazole treatment, although not significantly (P = 0.0509; paired *t* test) (**Figure 3B**). A representation of all rabbit-matched vitreous AUC data after both treatments is shown in **Figure 3C**.

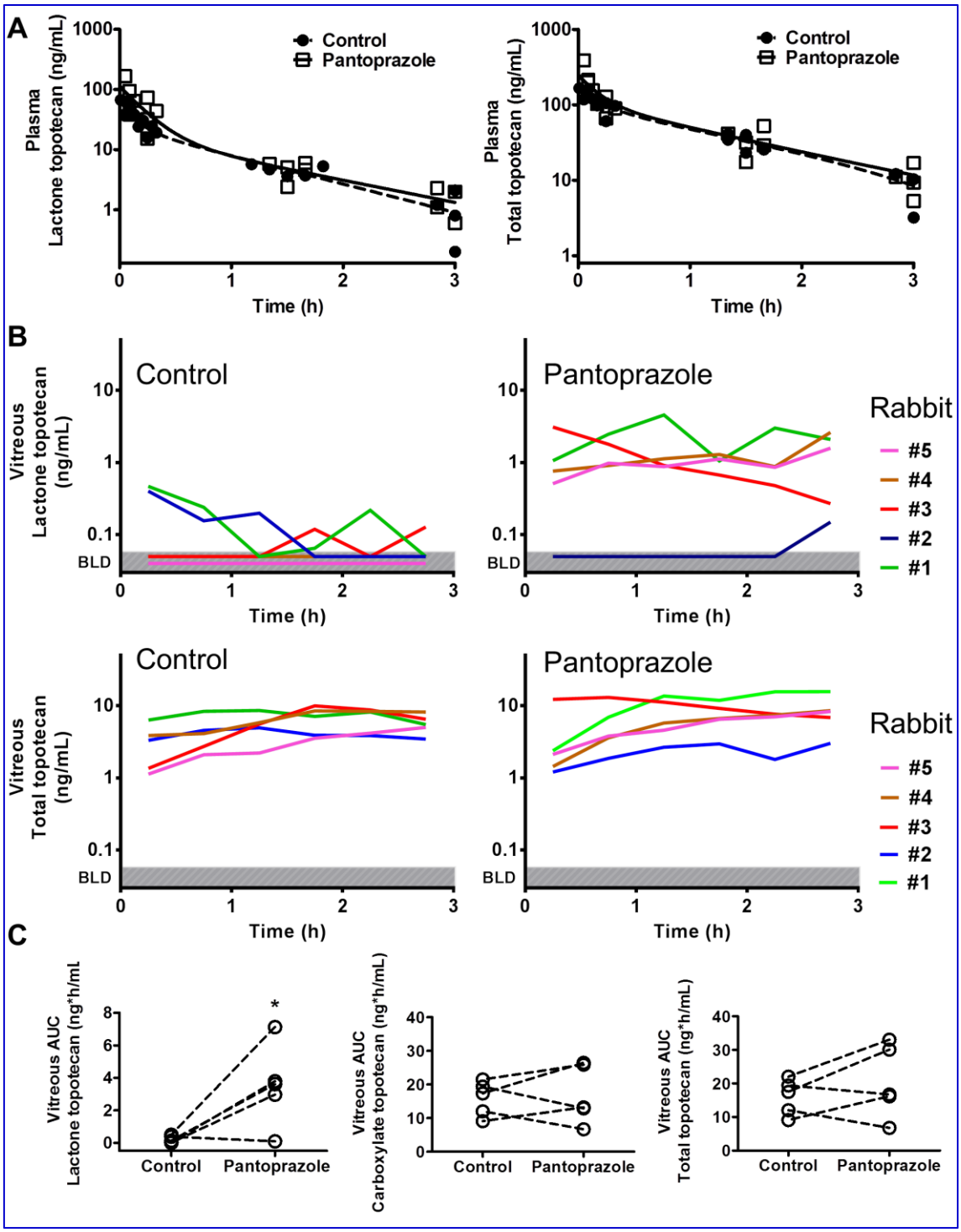

Figure 3. Effect of pantoprazole on topotecan plasma and vitreous distribution in rabbits. A) Plasma concentration-time profiles of unbound topotecan lactone (left panel) or total (right panel) in the absence (control) or presence of pantoprazole treatment. Dots are individual plasma concentration data obtained from 5 rabbits; each rabbit was bled 4 times. Curves were obtained upon fitting the data to a two phase decay model in Graphpad. B) Vitreous dialysates concentration-time profiles of unbound topotecan

lactone (top panels) or total (bottom panels) in the absence (Control) or presence of pantoprazole treatment (Pantoprazole). Concentration data obtained in 30 min intervals are represented for each of the 5 rabbits, identified with colors, and connected with lines at the median times of each interval. Data represented into the shadowed area are those below the limit of detection (BLD). C) Pairwise comparison of unbound vitreous *AUC* of topotecan lactone (left panel), carboxylate (central panel) and total (right panel) in the absence (control) or presence of pantoprazole. Lines connect data obtained from the same animal (5 rabbits in which both experiments were performed). *P = 0.040; paired *t* test.

AUCs of unbound lactone and total topotecan in vitreous and plasma obtained from each individual experiment are displayed in the **Supplemental Table**. Lactone topotecan $AUC_{u,vitreous}$ was significantly increased upon pantoprazole treatment (P = 0.040; paired *t* test), while plasma exposure ($AUC_{u,plasma}$) was not significantly modified (P = 0.182; paired *t* test). Median lactone topotecan vitreous-to-plasma *AUC* ratio (i.e., $P_{vitreous}$), expressed as percentage, was 6.4% (range 0.38-9.4%) after pantoprazole, significantly higher as compared to the topotecan alone treatment ($P_{vitreous}$ = 0.55%; range 0.00-1.6%; P = 0.029; paired *t* test). Total unbound topotecan *AUCs* in plasma and vitreous were not significantly different between both treatments (P = 0.457 and P = 0.277, respectively; paired *t* test).

Thus, from the rabbit microdialysis experiments it could be concluded that pantoprazole increased significantly the distribution of unbound topotecan lactone in the rabbit vitreous, while plasma exposures were not significantly altered.

Effect of pantoprazole on topotecan distribution in mouse vitreous and retina. Because mice are a more suitable model than the rabbit for studies of preclinical retinoblastoma, we next performed ocular pharmacokinetic

experiments in nude mice. In mice without tumors, $C_{ss,plasma}$ (mean ± SD) achieved 60.8 ± 17.6 and 94.7 ± 36.6 ng/mL for lactone and total topotecan, respectively. Plasma levels were not significantly altered by the presence of pantoprazole (P = 0.944 and P = 0.913) **(Figure 4A)**. $C_{ss,vitreous}$ of topotecan lactone in pantoprazole-treated mice increased 47%, from 22.0 ± 3.5 to 32.3 ± 8.7 (P = 0.0217) as compared to control mice. Total topotecan in the vitreous increased 52% (P = 0.0039). $C_{ss,retina}$ increased 26% for lactone (P = 0.2703) and 31% for total topotecan (P = 0.1021) (**Figure 4A**).

Topotecan penetration of the vitreous ($P_{vitreous}$) was significantly increased in mice upon the co-administration of pantoprazole (P = 0.0246 and P = 0.0064 for lactone and total, respectively) (**Figure 4B**).

Pantoprazole concentration-time curves in mouse plasma, vitreous and retina are shown in **Figure 4C**. Achieved C_{max} were 109 ± 23, 8.51 ± 1.74 and 49.4 ± 8.5 µM (mean and SD) in plasma, vitreous and retina, respectively. Pantoprazole concentrations were below the limit of quantification in retina and vitreous at 2 h.

We did not detect significant changes in the physiologic pH of mouse vitreous (mean pH = 7.58; range 7.38-7.78) or blood (mean pH = 7.42; range 7.36-7.47) upon 50 mg/kg pantoprazole treatment (**Supplemental Figure 3A**). *In vitro*, pH values of culture medium did not change due to the presence of pantoprazole in the range 2.5-2000 µM (**Supplemental Figure 3B**). Fluorescence of HSJD-RBT-2 cells did not change upon incubation with pantoprazole (2.5-500 µM) and FITC-dextran. Cells incubated with 2000 µM pantoprazole (not clinically relevant

concentration) showed higher fluorescence signal indicating an increment in the endosomal pH value (**Supplemental Figure 3C**).

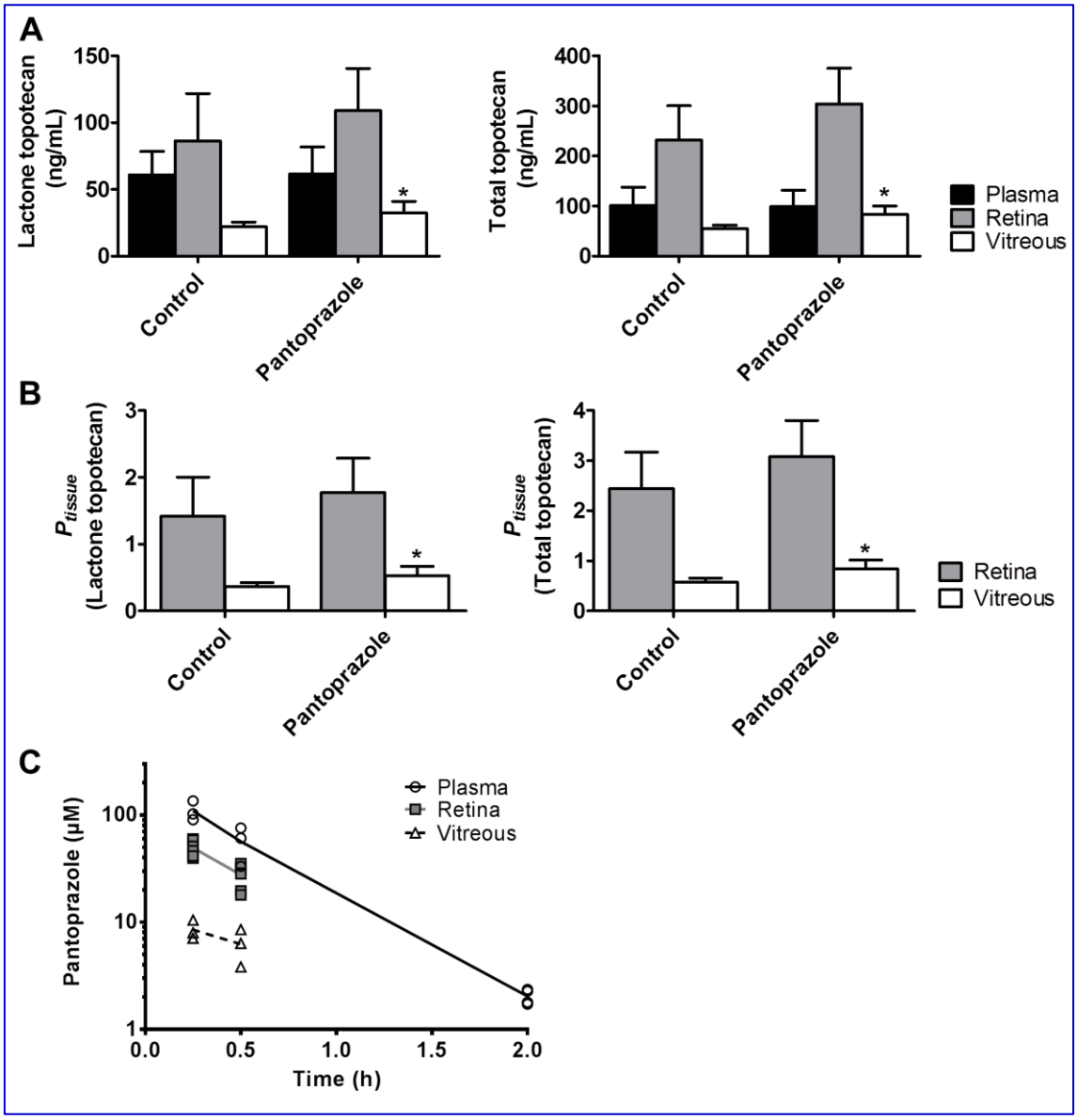

Figure 4. Effect of pantoprazole on topotecan penetration of vitreous and retina in nude mice. A. $C_{ss,tissue}$ (retina or vitreous) and $C_{ss,plasma}$ achieved for lactone and total topotecan. B. Extent of penetration of tissue (P_{retina} and $P_{vitreous}$) by lactone and total topotecan. Values are mean ± SD from 3 to 6 samples. *Significant difference as compared to control (Student's *t* test). C. Pantoprazole concentration-time data in mice after 50 mg/kg pantoprazole i.p.

Effect of pantoprazole on the distribution of topotecan in an intraocular retinoblastoma xenograft. The patient-derived xenograft HSJD-RBT-2 allows studying drug penetration of intraocular tumors at advanced stage, in which the whole content of the posterior segment of the eye is replaced by the engrafted tumor [28]. Topotecan tumor concentrations in animals with intraocular xenografts did not increase significantly with pantoprazole (P = 0.475 and P = 0.357 for lactone and total, respectively) (**Figure 5A**). P_{tumor} values remained similar as well (P = 0.399 and P = 0.486) (**Figure 5B**).

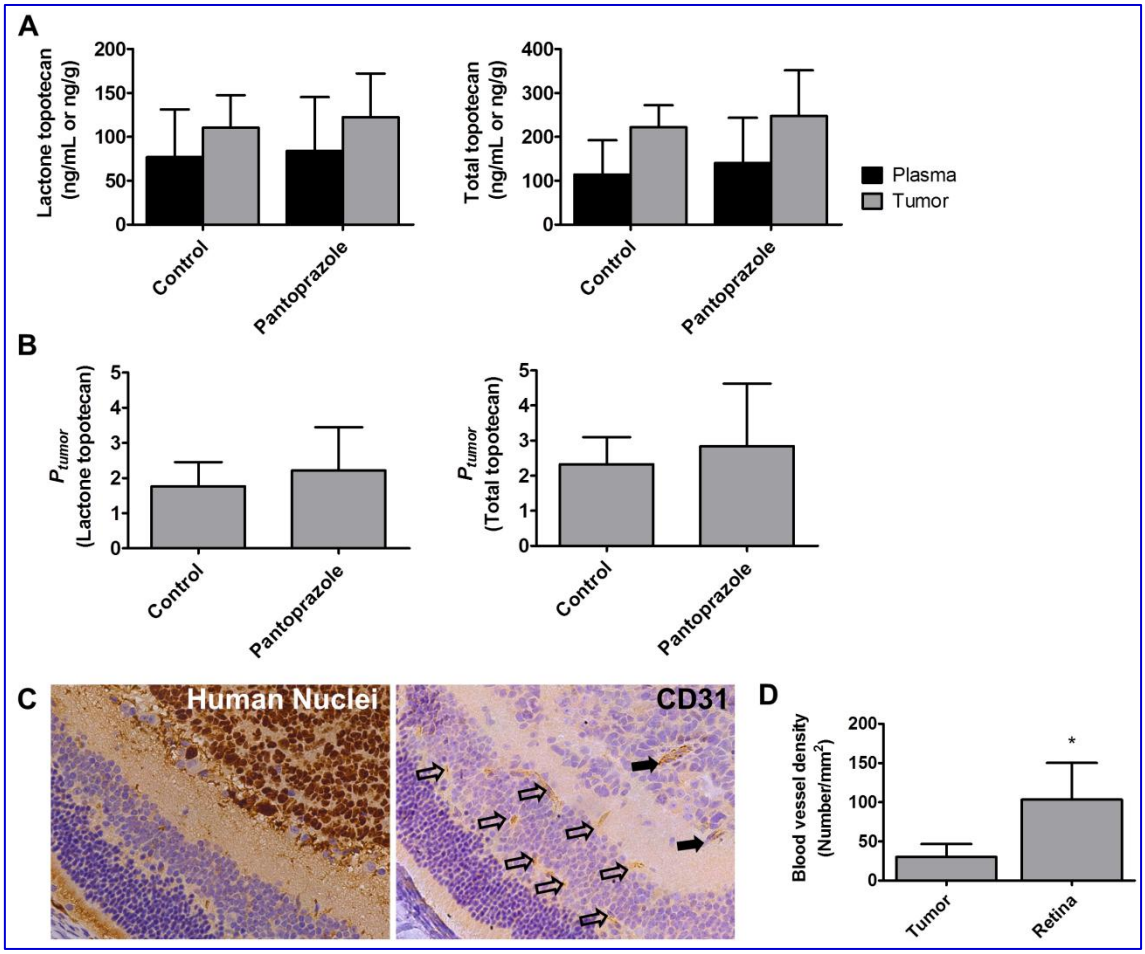

Figure 5. Effect of pantoprazole on topotecan penetration of orthotopic retinoblastoma xenograft HSJD-RBT-2 in nude mice. A. $C_{ss,tumor}$ and $C_{ss,plasma}$ achieved for lactone and total topotecan. B. Extent of penetration of tumor (P_{tumor}) by lactone and total topotecan. Values in columns are mean ± SD from 3 to 6 samples. C. Immunostaining of engrafted human tumors in the mouse eye. Human retinoblastoma cells nuclei into the

tumor bulk are stained in brown in the left picture, next to inner and outer nuclear layers (stained in blue) of the mouse retina. CD-31-positive vessels were counted in tumors (black arrows) and in the mouse retina (empty arrows). D. Blood vessel density in tumor and retinal areas of mouse eyes with engrafted tumors. Values in columns are mean ± SD from 4 quantifications. *P = 0.0253; Student's *t* test.

Because the tumor vasculature affects drug delivery [39], we stained retinal and tumor vessels in FFPE sections of HSJD-RBT-2 (**Figure 5C**). The density of CD-31 positive vessels in tumor areas was 3.4-fold lower than that in the retina (**Figure 5D**).

Effect of pantoprazole on topotecan antitumor efficacy in retinoblastoma xenografts. Median ocular survival in mice treated with *Control*, *Pantoprazole*, *Topotecan* and *Combination* was 46.0, 58.5, 82.0 and 82.5 days, respectively (**Figure 6**). Median ocular survival of *Topotecan* and *Combination* groups was significantly increased as compared to *Control* (P = 0.0003 and P < 0.0001), while *Pantoprazole* survival was not (P = 0.213). *Combination* did not improve survival as compared to *Topotecan* (P = 0.584). Despite the improvement in median ocular survival, the majority of tumors (90%) relapsed after topotecan treatment and required enucleation.

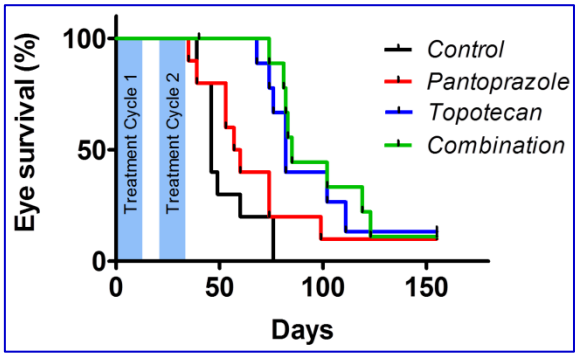

Figure 6. Ocular survival in mice treated with two cycles of topotecan (n = 8 eyes), pantoprazole (n = 10) or combination (n = 9), as compared to control eyes (n = 10).

Effect of pantoprazole on topotecan activity and accumulation *in vitro*. We found that all the retinoblastoma models were sensitive to topotecan in the low nanomolar range (median IC50 = 15.2 nM, range 4.39-53.1 nM; **Figure 7A**). Pantoprazole did not show antiproliferative effect against HSJD-RBT-2 cells at 500 µM (cell viability was 96.6 ± 22.4 % as compared to control cells; 2 h exposure). In HSJD-RBT-2 cells, combination of pantoprazole and 2 nM topotecan (IC10), increased the antiproliferative effect by 44.8 ± 13.3 % as compared to topotecan treatment alone (**Figure 7B**). This effect was not observed at the IC50 or IC90. In the presence of 500 µM pantoprazole, efflux rate of topotecan from HSJD-RBT-2 tumorspheres was decreased, leading to 23.9 ± 9.4 % higher intracellular topotecan amount after 30 min incubation (**Figure 7C**). Such effect was not significant at pantoprazole concentrations lower than 500 µM (**Figure 7D**).

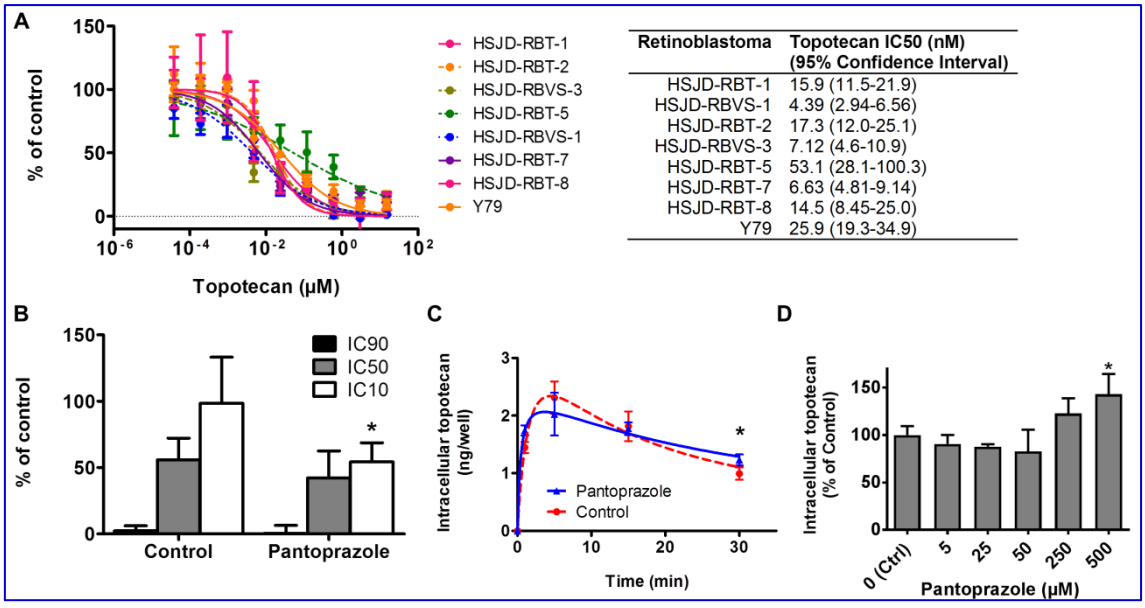

Retinoblastoma	Topotecan IC50 (nM) (95% Confidence Interval)
HSJD-RBT-1	15.9 (11.5-21.9)
HSJD-RBVS-1	4.39 (2.94-6.56)
HSJD-RBT-2	17.3 (12.0-25.1)
HSJD-RBVS-3	7.12 (4.6-10.9)
HSJD-RBT-5	53.1 (28.1-100.3)
HSJD-RBT-7	6.63 (4.81-9.14)
HSJD-RBT-8	14.5 (8.45-25.0)
Y79	25.9 (19.3-34.9)

Figure 7. Effect of pantoprazole on topotecan activity and accumulation in retinoblastoma cells. A) Antiproliferative activity of topotecan in patient-derived retinoblastoma models and the Y79 cell line. Values are expressed as % of MTS signal as compared to control untreated cells that were considered 100%. Median IC50

values (95% confidence intervals) are shown in the table. B) HSJD-RBT-2 cells are more sensitive to topotecan IC10 after pantoprazole treatment, as compared to control (no pantoprazole). Means and SD of 3 replicates are shown. *P = 0.0165; Student's *t* test. C) Topotecan accumulation in retinoblastoma HSJD-RBT-2 tumorspheres in the presence and absence (control) of pantoprazole. Values are expressed as the topotecan lactone amount accumulated in the tumorspheres in each well and quantified upon extraction with water and methanol. Curves were fitted with the Substrate Inhibition model in Graphpad Prism. *P = 0.046; Student's *t* test. D) Concentration-dependent effect of pantoprazole on topotecan accumulation in retinoblastoma HSJD-RBT-2 tumorspheres, in the range 0 (Control; Ctrl) to 500 µM pantoprazole. *P = 0.011; ANOVA.

Discussion

Chemotherapy agents carboplatin, vincristine, topotecan and their combinations, administered by the systemic route, have contributed to preserve eyes with vision in patients with retinoblastoma [40, 41]. However, their failure has been frequent in patients with retinoblastoma vitreous seeding, likely because these drugs do not penetrate to the avascular vitreous enough to achieve therapeutically active exposures [15]. In this study we provide proof of principle that pharmacological inhibition of the BRB leads to increased vitreous delivery of chemotherapy, through mechanisms that likely involve ABC transporters at the inner BRB.

The rabbit eye provides a similar proportion of volume between the aqueous and vitreous ocular compartments as compared to the human eye. Although the comparative anatomy of the rabbit and human retinal vasculature has been described in detail [35], our study confirmed for the first time by IHC that BCRP and P-gp are expressed in the rabbit retinal vasculature, which would be consistent with a functional BRB. The rabbit *BCRP* gene has been recently

cloned from the placenta [42]. Based on 86% analogy between human and rabbit BCRP aminoacid sequences, we predicted that the antibody BXP-21 would recognize rabbit BCRP [42]. To further demonstrate the specificity of the antibodies, we showed staining of BCRP and P-gp in the rabbit BBB vessels and in the apical side of the choroid plexus ependymal cells, following a similar pattern as compared to murine models [20]. BCRP and P-gp positivity of retinal vessels in the luminal side is consistent with the location of the transporter previously demonstrated in mouse retinal vessels, and rabbit BCRP shows affinity for the same substrates as human and mouse BCRP [5, 42]. Thus, the rabbit may provide a useful BRB model in ocular pharmacokinetic studies, and also a suitable BBB model.

The function of the human BRB is largely unknown and the findings in the rabbit and mouse BRB models should be translated cautiously to humans. A recent radio-imaging study in humans has confirmed that P-gp inhibition leads to accumulation of the P-gp substrate verapamil in the human retina [11]. Clinical translation of our results should also consider that although BCRP is expressed by rabbits and rats at the retinal vasculature, it is poorly expressed at the human inner BRB of the healthy eye [13, 43]. Thus, additional studies on the human BRB will be needed, or alternative animal models to reproduce it more accurately.

Our selection of topotecan as a model drug was justified by its clinical relevance in ocular oncology [44]. The activity of systemic topotecan was observed two decades ago in a few patients with intraocular retinoblastoma [45-47]. More recently, topotecan was evaluated formally in two phase II clinical trials, in combination with vincristine and carboplatin, showing manageable toxicity and

significant activity in most patients [41, 48]. Another reason to select topotecan for our study was that our previous preclinical pharmacokinetic studies at high systemic dose confirmed limited vitreous distribution of its lactone form [19, 27].

Pantoprazole has been shown to modify drug distribution in tumors by two mechanisms, either by the inhibition of efflux transporters [21] or by induction of changes in the endosomal pH of the tumor cells [23]. Our study supports that the inhibition of the inner BRB was the most likely mechanism by which pantoprazole modified topotecan vitreous distribution in rabbits and mice. In addition, ABC transporters have a higher affinity for lactone topotecan than for the carboxylate counterpart [37]. Thus, our finding of increased lactone (and not carboxylate) exposure in the rabbit vitreous supported further the proposed mechanism of pantoprazole activity through inhibition of the efflux transporters at the BRB. We speculate that topotecan lactone levels achieved in the rabbit vitreous would have reached potentially active concentrations in 3 out of 8 retinoblastoma models (those with IC50 lower than 10 nM; **Figure 7**) upon co-administration of pantoprazole.

To improve our ability to extrapolate these results to the clinical scenario we characterized the pharmacokinetics of pantoprazole in mice. The dosage in the mouse study (50 mg/kg) was limited by the observation of acute toxicity when combined with topotecan at higher pantoprazole dosages. In human patients, a single i.v. dose of 240 mg, combined with doxorubicin, achieves a concentration of 100 µM in plasma [24]. The concentration of pantoprazole in mouse plasma was in a similar range in our study, suggesting that the reported clinical dosage could reach potentially active concentrations at the human BRB. At such systemic exposure (C_{max} 100 µM) in mice, concentrations in the mouse retina

(C_{max} 50 µM) inhibited the BRB, leading to increased topotecan exposure in the vitreus. Although we did not test whether this concentration inhibited a BRB model *in vitro*, previous published work using membrane vesicles from Sf9 cells infected with a baculovirus containing human BCRP showed that pantoprazole reduced 50% of BCRP function at 10 µM and 90% at 50 µM [21]. We did not perform a pharmacokinetic study of pantoprazole in rabbits, although their dosage calculated in mg/kg was in a similar range as compared to the mentioned clinical trial.

Because the presence of intraocular tumors with their own blood supply may modify or destroy the normal retinal vasculature, we studied the BRB proteins in the tumor and retinal vessels of a small cohort of enucleated patients. Our finding of BCRP and P-gp-positive tumor vasculature was consistent with previous findings in human retinoblastoma treated by primary enucleation [49]. In our study, it is likely that tumor vessels expressed ABC transporters also as a response to treatments, because most of these eyes –with the exception of Patient 7- were exposed to intensive local chemotherapy [28]. In fact, BCRP and P-gp expression are upregulated in the endothelial cells of the BBB upon pretreatment with xenobiotics [50]. Also, P-gp has been previously found up-regulated in tumor endothelial cells as compared to normal endothelial cells, conferring resistance to paclitaxel [51].

Our data showed that the mouse model without tumor reproduced partially the rabbit data on the interaction of topotecan and pantoprazole. Differences such as the higher topotecan $P_{vitreous}$ observed in mice could be attributed, among other reasons, to the dissection of the mouse eye, which was performed post-mortem. In such conditions, the local amounts of drug may be redistributed in

the tissues due to cessation of the active blood clearance [19]. In contrast, ocular microdialysis in alive rabbits might have conserved to a greater extent the physiological clearance mechanisms in the vitreous [6]. Because topotecan concentrations in the mouse retinas showed higher variability than the ones in the vitreous, with our sample size we could not confirm whether the effect of pantoprazole to increase drug distribution in the retina was significant, as it was expected according to recently published data [11]. Variability was likely due to methodological limitations in our technique to dissect and process small tissue samples.

Inhibitors of drug efflux transporters might have an additional impact at the tumor cell level, to increase intracellular accumulation and efficacy of substrate drugs [29]. We addressed this question by performing studies of BCRP and P-gp expression in our tumor models and in the patients from which the models were developed. We confirmed that such expression was variable among the retinoblastoma models in culture, and it was low or even undetectable in some of them, which is consistent with the IHC findings of the group at St. Jude Children's Research Hospital in a cohort of 62 enucleated eyes. They reported 77% of patient tumors stained positive at least for one ABC transporter, 19% of them BCRP-positive and 27% of them P-gp-positive [52]. In agreement with the function of efflux transporters at the tumor cell level, we found a bell-shaped accumulation curve of topotecan in HSJD-RBT-2 tumorspheres in culture (**Figure 7C**). Such shape could be the consequence of a fast uptake phase leading to intracellular topotecan accumulation, followed by active drug efflux that was slowed down by pantoprazole.

In vivo, intraocular retinoblastoma xenografts in mice reproduce the main histological features of the original human tumor [28]. Limitations of this model might be related to the spatial relation of the tumor and the remaining ocular compartments, since the xenograft grows promptly to load the whole (and limited) volume of the posterior segment of the mouse eye. Also, the vascular count of the orthotopic xenograft was consistent with the previous observation that retinoblastoma cells grow as avascular masses into the mouse eye, impeding the efficacy of systemic chemotherapy [53]. Thus, it is likely that the combination therapy failed to increase topotecan distribution and ocular survival in our study due to such limitations of the model. In addition, our *in vitro* studies showed that pantoprazole needs to achieve at least 500 µM to inhibit drug efflux at the tumor cell level (**Figure 7D**). Even in the hypothetical context of an open BRB, it would have been unfeasible to achieve such concentration in our model.

The clinical question whether pharmacological modulators of ABC transporters could enhance the potency of retinoblastoma chemotherapy regimens was addressed by the group at the University of Toronto [54]. They found that P-gp was increased in a set of human retinoblastoma tumors [55] and designed a clinical strategy to inhibit P-gp function in retinoblastoma patients receiving systemic chemotherapy with concomitant cyclosporin A as P-gp inhibitor [54]. The results of their clinical studies did not support further clinical application [56]. Relevant preclinical studies on this specific approach are still lacking because the hypothesis on the effect of cyclosporine A on ocular drug distribution was tested in rabbits using carboplatin [57], which is a non-P-gp substrate [58].

To conclude, ours is the first work to modulate concentrations of an anticancer drug in the vitreous upon the systemic administration of a drug efflux transporter inhibitor. Further preclinical work should address whether our results are reproducible in other animal models, or whether local administration of the transporter inhibitor leads to more pronounced effects on the BRB function.

Acknowledgements

AMC acknowledges funding from ISCIII-FEDER (CP13/00189), MINECO (Retos program; Cure4RB project RTC-2015-4319-1) and European Union Seventh Framework Programme (FP7/2007-2013) under Marie Curie International Reintegration Grant (PIRG-08-GA-2010-276998). GLC and PS acknowledge funding from Fund for Ophthalmic Knowledge, New York, NY. CARP was funded by the Fred-Hollows Foundation (Sydney, Australia) through the ICO fellowship board (Homburg/Saar, Germany). This work was supported by the Xarxa de Bancs de Tumors de Catalunya (XBTC) sponsored by Pla Director d'Oncologia de Catalunya. We thank Maria Jesus Nagel for technical assistance.

References

[1] H. Dimaras, T.W. Corson, D. Cobrinik, A. White, J. Zhao, F.L. Munier, D.H. Abramson, C.L. Shields, G.L. Chantada, F. Njuguna, B.L. Gallie, Retinoblastoma, Nature reviews. Disease primers, 1 (2015) 15021.

[2] L.A. Murphree, Intraocular retinoblastoma: the case for a new group classification, Ophthalmol Clin North Am, 18 (2005) 41-53, viii.

[3] F.L. Munier, Classification and Management of Seeds in Retinoblastoma. Ellsworth Lecture Ghent August 24th 2013, Ophthalmic Genetics, 35 (2014) 193-207.

[4] K. Hosoya, M. Tachikawa, The inner blood-retinal barrier: molecular structure and transport biology, Adv Exp Med Biol, 763 (2012) 85-104.

[5] T. Asashima, S. Hori, S. Ohtsuki, M. Tachikawa, M. Watanabe, C. Mukai, S. Kitagaki, N. Miyakoshi, T. Terasaki, ATP-binding cassette transporter G2 mediates the efflux of phototoxins on the luminal membrane of retinal capillary endothelial cells, Pharm Res, 23 (2006) 1235-1242.

[6] E.M. del Amo, A.-K. Rimpelä, E. Heikkinen, O.K. Kari, E. Ramsay, T. Lajunen, M. Schmitt, L. Pelkonen, M. Bhattacharya, D. Richardson, A. Subrizi, T. Turunen, M. Reinisalo, J. Itkonen, E. Toropainen, M. Casteleijn, H. Kidron, M. Antopolsky, K.-S. Vellonen, M. Ruponen, A. Urtti, Pharmacokinetic aspects of retinal drug delivery, Progress in Retinal and Eye Research, 57 (2017) 134-185.

[7] D.H. Abramson, C.L. Shields, F.L. Munier, G.L. Chantada, Treatment of Retinoblastoma in 2015: Agreement and Disagreement, JAMA ophthalmology, 133 (2015) 1341-1347.

[8] A. Parareda, J. Catala, A.M. Carcaboso, T. Sola, O. Cruz, J. Diaz, H. Salvador, C. de Torres, A. Alvarez-Sampons, M. Sunol, J. Vinent, L. Guimaraens, J. Prat, J. Mora, Intra-arterial chemotherapy for retinoblastoma. Challenges of a prospective study, Acta Ophthalmol, 92 (2014) 209-215.

[9] F.L. Munier, M.C. Gaillard, A. Balmer, S. Soliman, G. Podilsky, A.P. Moulin, M. Beck-Popovic, Intravitreal chemotherapy for vitreous disease in retinoblastoma revisited: from prohibition to conditional indications, Br J Ophthalmol, 96 (2012) 1078-1083.

[10] H. Chapy, B. Saubamea, N. Tournier, F. Bourasset, F. Behar-Cohen, X. Decleves, J.M. Scherrmann, S. Cisternino, Blood-brain and retinal barriers show dissimilar ABC transporter impacts and concealed effect of P-glycoprotein on a novel verapamil influx carrier, Br J Pharmacol, 173 (2016) 497-510.

[11] M. Bauer, R. Karch, N. Tournier, S. Cisternino, W. Wadsak, M. Hacker, P. Marhofer, M. Zeitlinger, O. Langer, Assessment of P-Glycoprotein Transport Activity at the Human Blood-Retina Barrier with (R)-11C-Verapamil PET, J Nucl Med, 58 (2017) 678-681.

[12] H. Chapy, P. Andre, X. Decleves, J.M. Scherrmann, S. Cisternino, A polyspecific drug/proton antiporter mediates diphenhydramine and clonidine transport at the mouse blood-retinal barrier, Br J Pharmacol, 172 (2015) 4714-4725.

[13] A. Dahlin, E. Geier, S.L. Stocker, C.D. Cropp, E. Grigorenko, M. Bloomer, J. Siegenthaler, L. Xu, A.S. Basile, D.D. Tang-Liu, K.M. Giacomini, Gene expression profiling of transporters in the solute carrier and ATP-binding cassette superfamilies in human eye substructures, Mol Pharm, 10 (2013) 650-663.

[14] H. Carol, P.J. Houghton, C.L. Morton, E.A. Kolb, R. Gorlick, C.P. Reynolds, M.H. Kang, J.M. Maris, S.T. Keir, A. Watkins, M.A. Smith, R.B. Lock, Initial

testing of topotecan by the pediatric preclinical testing program, Pediatr Blood Cancer, 54 (2010) 707-715.

[15] N.A. Laurie, J.K. Gray, J. Zhang, M. Leggas, M. Relling, M. Egorin, C. Stewart, M.A. Dyer, Topotecan combination chemotherapy in two new rodent models of retinoblastoma, Clin Cancer Res, 11 (2005) 7569-7578.

[16] K.M. Nemeth, S. Federico, A.M. Carcaboso, Y. Shen, P. Schaiquevich, J. Zhang, M. Egorin, C. Stewart, M.A. Dyer, Subconjunctival carboplatin and systemic topotecan treatment in preclinical models of retinoblastoma, Cancer, 117 (2011) 421-434.

[17] R. Garcia-Carbonero, J.G. Supko, Current perspectives on the clinical experience, pharmacology, and continued development of the camptothecins, Clin Cancer Res, 8 (2002) 641-661.

[18] M. Leggas, Y. Zhuang, J. Welden, Z. Self, C.M. Waters, C.F. Stewart, Microbore HPLC method with online microdialysis for measurement of topotecan lactone and carboxylate in murine CSF, J Pharm Sci, 93 (2004) 2284-2295.

[19] A.M. Carcaboso, G.F. Bramuglia, G.L. Chantada, A.C. Fandino, D.A. Chiappetta, M.T. de Davila, M.C. Rubio, D.H. Abramson, Topotecan vitreous levels after periocular or intravenous delivery in rabbits: an alternative for retinoblastoma chemotherapy, Invest Ophthalmol Vis Sci, 48 (2007) 3761-3767.

[20] Y. Zhuang, C.H. Fraga, K.E. Hubbard, N. Hagedorn, J.C. Panetta, C.M. Waters, C.F. Stewart, Topotecan central nervous system penetration is altered by a tyrosine kinase inhibitor, Cancer Res., 66 (2006) 11305-11313.

[21] P. Breedveld, N. Zelcer, D. Pluim, O. Sonmezer, M.M. Tibben, J.H. Beijnen, A.H. Schinkel, O. van Tellingen, P. Borst, J.H. Schellens, Mechanism of the pharmacokinetic interaction between methotrexate and benzimidazoles: potential role for breast cancer resistance protein in clinical drug-drug interactions, Cancer Res, 64 (2004) 5804-5811.

[22] S. Kunimatsu, T. Mizuno, M. Fukudo, T. Katsura, Effect of P-glycoprotein and breast cancer resistance protein inhibition on the pharmacokinetics of sunitinib in rats, Drug Metab Dispos, 41 (2013) 1592-1597.

[23] K.J. Patel, C. Lee, Q. Tan, I.F. Tannock, Use of the proton pump inhibitor pantoprazole to modify the distribution and activity of doxorubicin: a potential strategy to improve the therapy of solid tumors, Clin Cancer Res, 19 (2013) 6766-6776.

[24] I. Brana, A. Ocana, E.X. Chen, A.R. Razak, C. Haines, C. Lee, S. Douglas, L. Wang, L.L. Siu, I.F. Tannock, P.L. Bedard, A phase I trial of pantoprazole in combination with doxorubicin in patients with advanced solid tumors: evaluation of pharmacokinetics of both drugs and tissue penetration of doxorubicin, Invest New Drugs, 32 (2014) 1269-1277.

[25] M. Hammarlund-Udenaes, M. Friden, S. Syvanen, A. Gupta, On the rate and extent of drug delivery to the brain, Pharm Res, 25 (2008) 1737-1750.

[26] C. Monterrubio, S. Paco, M. Vila-Ubach, E. Rodriguez, R. Glisoni, C. Lavarino, P. Schaiquevich, A. Sosnik, J. Mora, A.M. Carcaboso, Combined Microdialysis-Tumor Homogenate Method for the Study of the Steady State Compartmental Distribution of a Hydrophobic Anticancer Drug in Patient-Derived Xenografts, Pharm Res, 32 (2015) 2889-2900.

[27] A.M. Carcaboso, D.A. Chiappetta, J.A. Opezzo, C. Hocht, A.C. Fandino, J.O. Croxatto, M.C. Rubio, A. Sosnik, D.H. Abramson, G.F. Bramuglia, G.L. Chantada, Episcleral implants for topotecan delivery to the posterior segment of the eye, Invest Ophthalmol Vis Sci, 51 (2010) 2126-2134.

[28] G. Pascual-Pasto, N.G. Olaciregui, M. Vila-Ubach, S. Paco, C. Monterrubio, E. Rodriguez, U. Winter, M. Batalla-Vilacis, J. Catala, H. Salvador, A. Parareda, P. Schaiquevich, M. Sunol, J. Mora, C. Lavarino, C. de Torres, G.L. Chantada, A.M. Carcaboso, Preclinical platform of retinoblastoma xenografts recapitulating human disease and molecular markers of dissemination, Cancer Lett, 380 (2016) 10-19.

[29] A.M. Carcaboso, M.A. Elmeliegy, J. Shen, S.J. Juel, Z.M. Zhang, C. Calabrese, L. Tracey, C.M. Waters, C.F. Stewart, Tyrosine kinase inhibitor gefitinib enhances topotecan penetration of gliomas, Cancer Res, 70 (2010) 4499-4508.

[30] L. Wang, P.J. McNamara, Stereoselective interaction of pantoprazole with ABCG2. I. Drug accumulation in rat milk, Drug Metab Dispos, 40 (2012) 1018-1023.

[31] A. Marchetti, E. Lelong, P. Cosson, A measure of endosomal pH by flow cytometry in Dictyostelium, BMC Research Notes, 2 (2009) 7.

[32] U. Winter, H.A. Mena, S. Negrotto, E. Arana, G. Pascual-Pasto, V. Laurent, M. Sunol, G.L. Chantada, A.M. Carcaboso, P. Schaiquevich, Schedule-Dependent Antiangiogenic and Cytotoxic Effects of Chemotherapy on Vascular Endothelial and Retinoblastoma Cells, PLoS One, 11 (2016) e0160094.

[33] M. Leggas, J.C. Panetta, Y. Zhuang, J.D. Schuetz, B. Johnston, F. Bai, B. Sorrentino, S. Zhou, P.J. Houghton, C.F. Stewart, Gefitinib modulates the function of multiple ATP-binding cassette transporters in vivo, Cancer Res, 66 (2006) 4802-4807.

[34] P.J. Houghton, G.S. Germain, F.C. Harwood, J.D. Schuetz, C.F. Stewart, E. Buchdunger, P. Traxler, Imatinib mesylate is a potent inhibitor of the ABCG2 (BCRP) transporter and reverses resistance to topotecan and SN-38 in vitro, Cancer Res, 64 (2004) 2333-2337.

[35] M. Vézina, Comparative Ocular Anatomy in Commonly Used Laboratory Animals, in: B.A. Weir, M. Collins (Eds.) Assessing Ocular Toxicology in Laboratory Animals, Humana Press, Totowa, NJ, 2013, pp. 1-21.

[36] S. Yousif, C. Marie-Claire, F. Roux, J.M. Scherrmann, X. Decleves, Expression of drug transporters at the blood-brain barrier using an optimized isolated rat brain microvessel strategy, Brain Res, 1134 (2007) 1-11.

[37] J. Shen, A.M. Carcaboso, K.E. Hubbard, M. Tagen, H.G. Wynn, J.C. Panetta, C.M. Waters, M.A. Elmeliegy, C.F. Stewart, Compartment-specific roles of ATP-binding cassette transporters define differential topotecan distribution in brain parenchyma and cerebrospinal fluid, Cancer Res, 69 (2009) 5885-5892.

[38] J. Lee, R.M. Pelis, Drug Transport by the Blood-Aqueous Humor Barrier of the Eye, Drug Metab Dispos, 44 (2016) 1675-1681.

[39] A.I. Minchinton, I.F. Tannock, Drug penetration in solid tumours, Nat Rev Cancer, 6 (2006) 583-592.

[40] R.C. Brennan, I. Qaddoumi, S. Mao, J. Wu, C.A. Billups, C.F. Stewart, M.E. Hoehn, C. Rodriguez-Galindo, M.W. Wilson, Ocular Salvage and Vision Preservation Using a Topotecan-Based Regimen for Advanced Intraocular Retinoblastoma, Journal of Clinical Oncology, 35 (2017) 72-77.

[41] I. Qaddoumi, C.A. Billups, M. Tagen, C.F. Stewart, J. Wu, K. Helton, M.B. McCarville, T.E. Merchant, R. Brennan, T.M. Free, V. Given, B.G. Haik, C. Rodriguez-Galindo, M.W. Wilson, Topotecan and vincristine combination is effective against advanced bilateral intraocular retinoblastoma and has manageable toxicity, Cancer, 118 (2012) 5663-5670.

[42] S. Halwachs, C. Kneuer, K. Gohlsch, M. Müller, V. Ritz, W. Honscha, The ABCG2 efflux transporter from rabbit placenta: Cloning and functional characterization, Placenta, 38 (2016) 8-15.

[43] P. Chen, H. Chen, X. Zang, M. Chen, H. Jiang, S. Han, X. Wu, Expression of efflux transporters in human ocular tissues, Drug Metab Dispos, 41 (2013) 1934-1948.

[44] P. Schaiquevich, A.M. Carcaboso, E. Buitrago, P. Taich, J. Opezzo, G. Bramuglia, G.L. Chantada, Ocular pharmacology of topotecan and its activity in retinoblastoma, Retina, 34 (2014) 1719-1727.

[45] R. Nitschke, J. Parkhurst, J. Sullivan, M.B. Harris, M. Bernstein, C. Pratt, Topotecan in pediatric patients with recurrent and progressive solid tumors: a Pediatric Oncology Group phase II study, J Pediatr Hematol Oncol, 20 (1998) 315-318.

[46] H. Frangoul, M.M. Ames, R.B. Mosher, J.M. Reid, M.D. Krailo, N.L. Seibel, D.W. Shaw, P.G. Steinherz, J.A. Whitlock, J.S. Holcenberg, Phase I study of topotecan administered as a 21-day continous infusion in children with

recurrent solid tumors: a report from the Children's Cancer Group, Clin Cancer Res, 5 (1999) 3956-3962.

[47] G.L. Chantada, A.C. Fandino, S.J. Casak, G. Mato, J. Manzitti, E. Schvartzman, Activity of topotecan in retinoblastoma, Ophthalmic Genet, 25 (2004) 37-43.

[48] R.C. Brennan, I. Qaddoumi, S. Mao, J. Wu, C.A. Billups, C.F. Stewart, M.E. Hoehn, C. Rodriguez-Galindo, M.W. Wilson, Ocular Salvage and Vision Preservation Using a Topotecan-Based Regimen for Advanced Intraocular Retinoblastoma, Journal of Clinical Oncology, 35 (2017) 72-77.

[49] M.W. Wilson, C.H. Fraga, C.E. Fuller, C. Rodriguez-Galindo, J. Mancini, N. Hagedorn, M.L. Leggas, C.F. Stewart, Immunohistochemical detection of multidrug-resistant protein expression in retinoblastoma treated by primary enucleation, Invest Ophthalmol Vis Sci, 47 (2006) 1269-1273.

[50] S. Yousif, C. Chaves, S. Potin, I. Margaill, J.M. Scherrmann, X. Decleves, Induction of P-glycoprotein and Bcrp at the rat blood-brain barrier following a subchronic morphine treatment is mediated through NMDA/COX-2 activation, J Neurochem, 123 (2012) 491-503.

[51] K. Hida, K. Akiyama, N. Ohga, N. Maishi, Y. Hida, Tumour endothelial cells acquire drug resistance in a tumour microenvironment, Journal of Biochemistry, 153 (2013) 243-249.

[52] M.W. Wilson, C.H. Fraga, C. Rodriguez-Galindo, N. Hagedorn, M.L. Leggas, C. Stewart, Expression of the multi-drug resistance proteins and the pregnane X receptor in treated and untreated retinoblastoma, Current eye research, 34 (2009) 386-394.

[53] L. White, C.J. Gomer, D.R. Doiron, B.C. Szirth, Ineffective photodynamic therapy (PDT) in a poorly vascularized xenograft model, Br J Cancer, 57 (1988) 455-458.

[54] H.S. Chan, G. DeBoer, J.J. Thiessen, A. Budning, J.E. Kingston, J.M. O'Brien, G. Koren, E. Giesbrecht, G. Haddad, Z. Verjee, J.L. Hungerford, V. Ling, B.L. Gallie, Combining cyclosporin with chemotherapy controls intraocular retinoblastoma without requiring radiation, Clin Cancer Res, 2 (1996) 1499-1508.

[55] H.S. Chan, P.S. Thorner, G. Haddad, B.L. Gallie, Multidrug-resistant phenotype in retinoblastoma correlates with P-glycoprotein expression, Ophthalmology, 98 (1991) 1425-1431.

[56] H.S. Chan, Y. Lu, T.M. Grogan, G. Haddad, D.R. Hipfner, S.P. Cole, R.G. Deeley, V. Ling, B.L. Gallie, Multidrug resistance protein (MRP) expression in retinoblastoma correlates with the rare failure of chemotherapy despite cyclosporine for reversal of P-glycoprotein, Cancer Res, 57 (1997) 2325-2330.

[57] T.W. Wilson, H.S. Chan, G.M. Moselhy, D.D. Heydt, Jr., C.M. Frey, B.L. Gallie, Penetration of chemotherapy into vitreous is increased by cryotherapy and cyclosporine in rabbits, Arch Ophthalmol, 114 (1996) 1390-1395.

[58] D.W. Shen, L.M. Pouliot, M.D. Hall, M.M. Gottesman, Cisplatin resistance: a cellular self-defense mechanism resulting from multiple epigenetic and genetic changes, Pharmacol Rev, 64 (2012) 706-721.

Figure(s)

Click here to download high resolution image

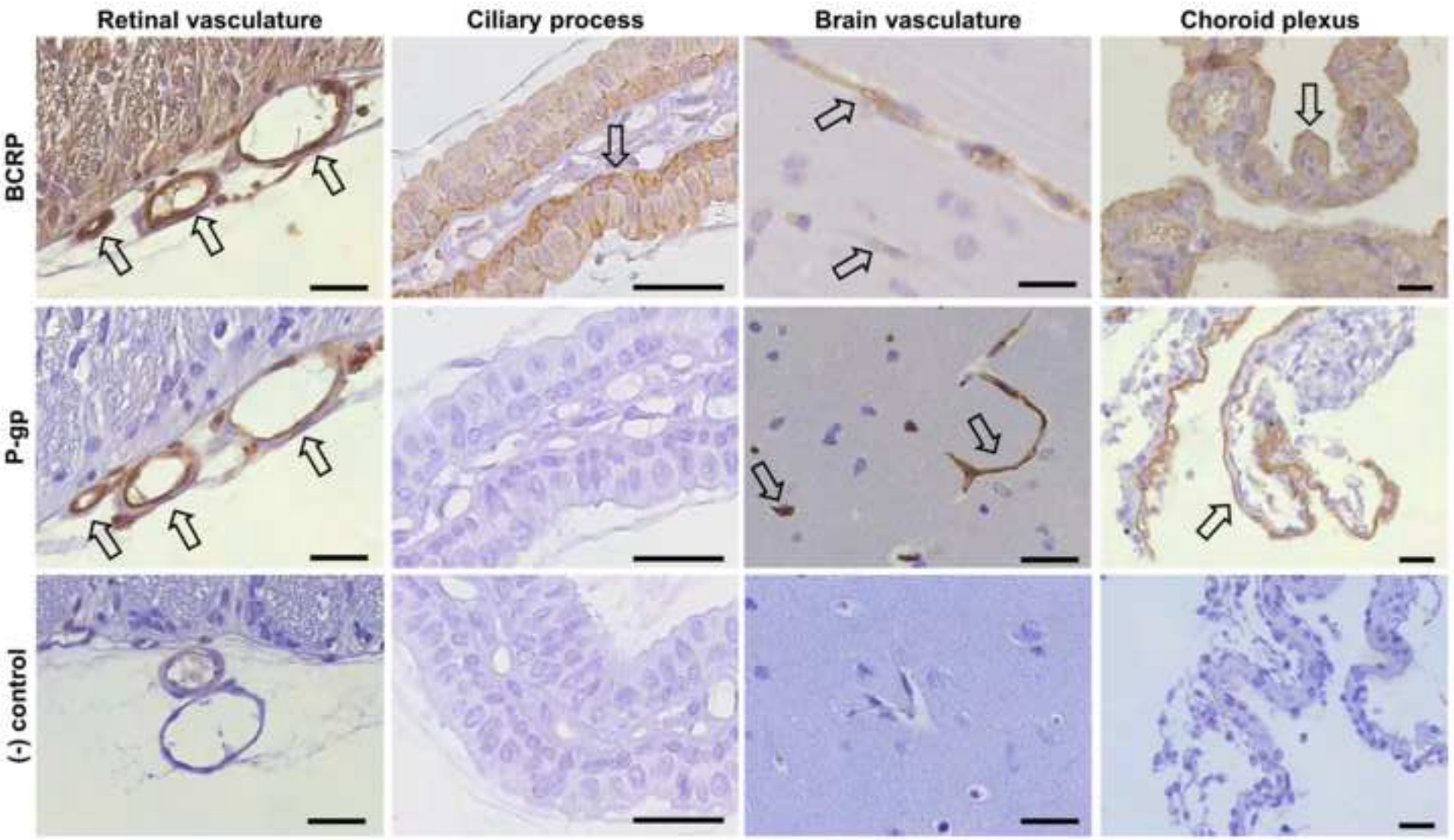

Figure(s)

Click here to download high resolution image

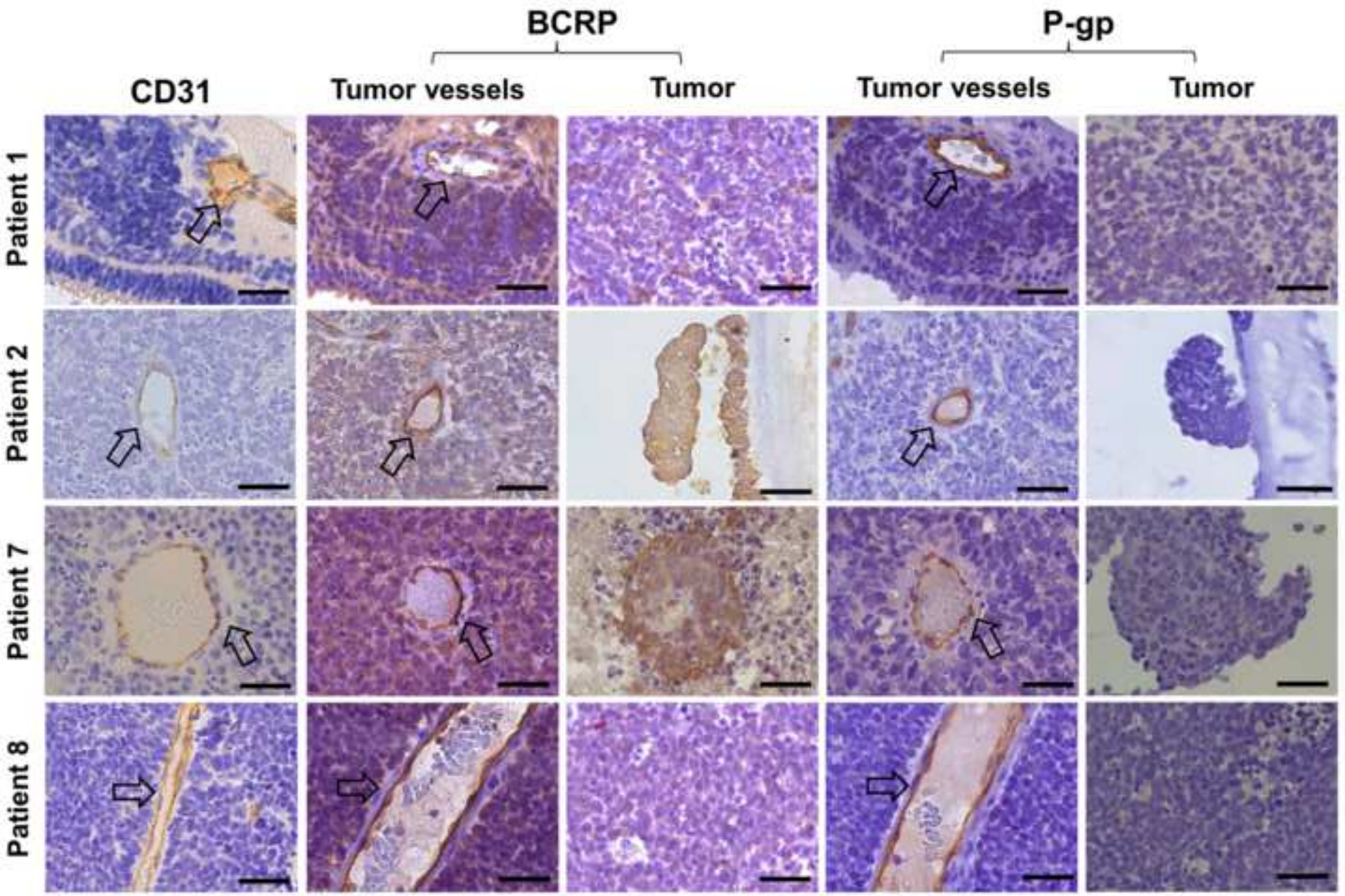

Figure(s)

Click here to download high resolution image

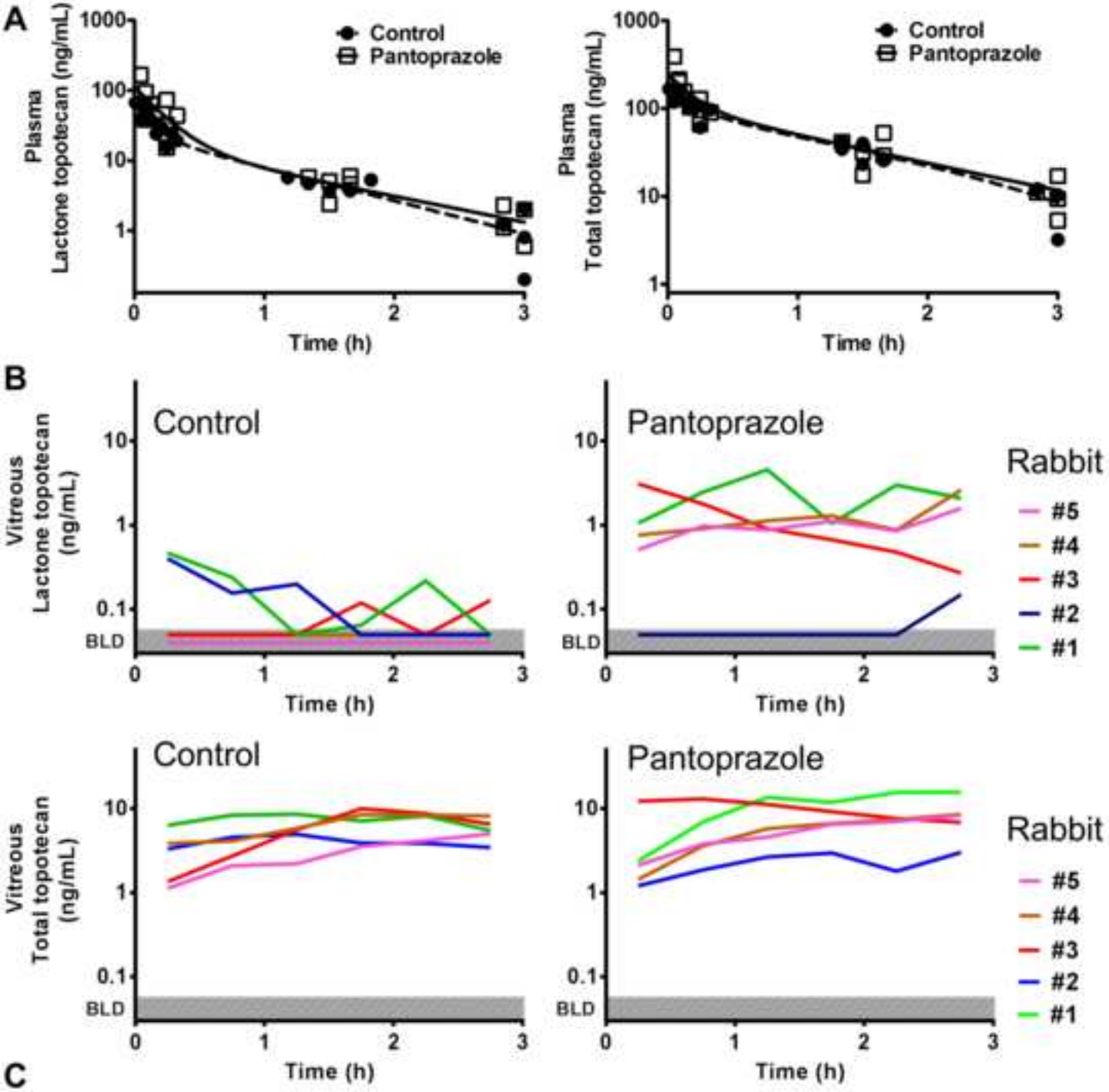

Figure(s)

Click here to download high resolution image

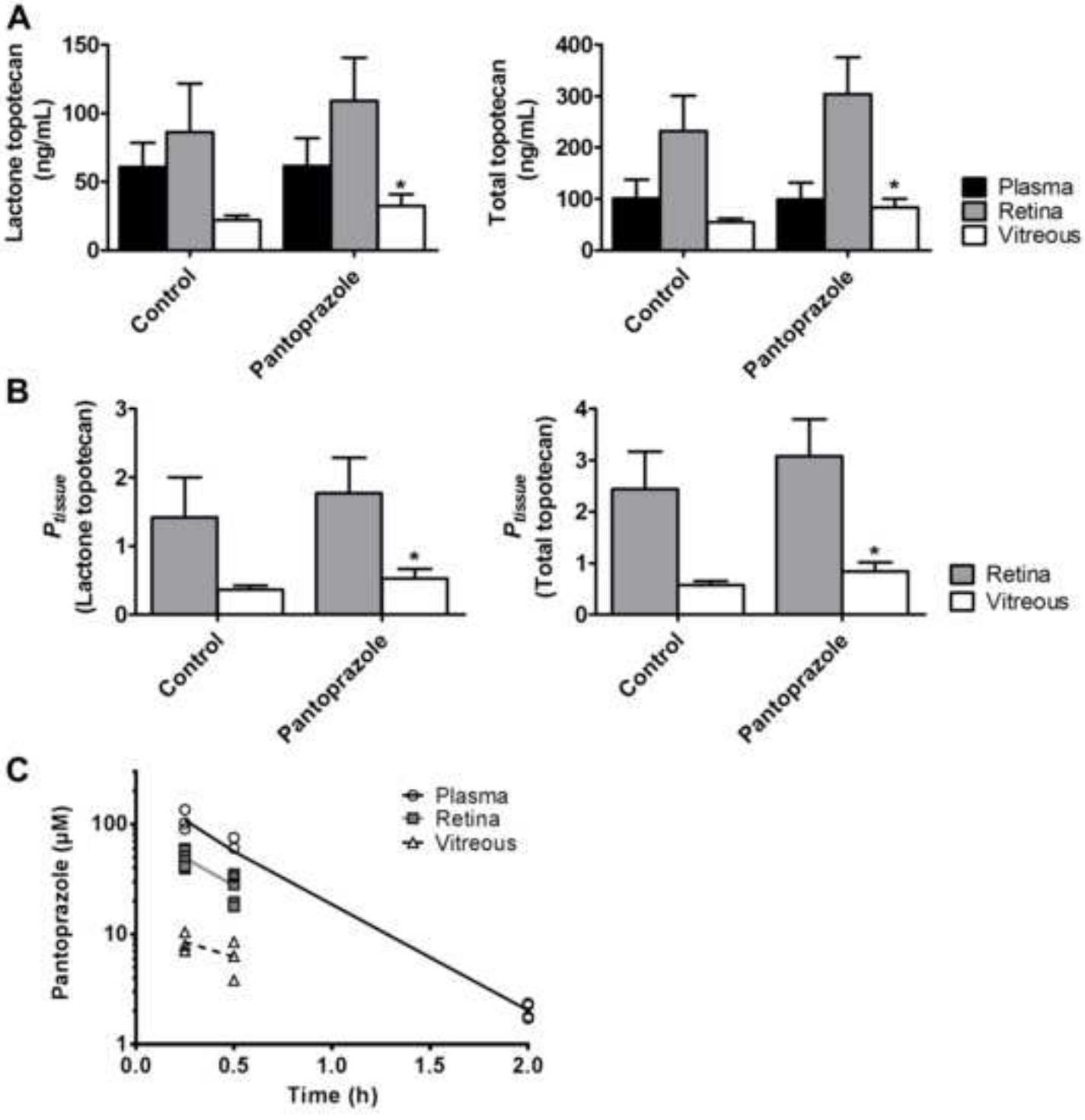

Figure(s)

Click here to download high resolution image

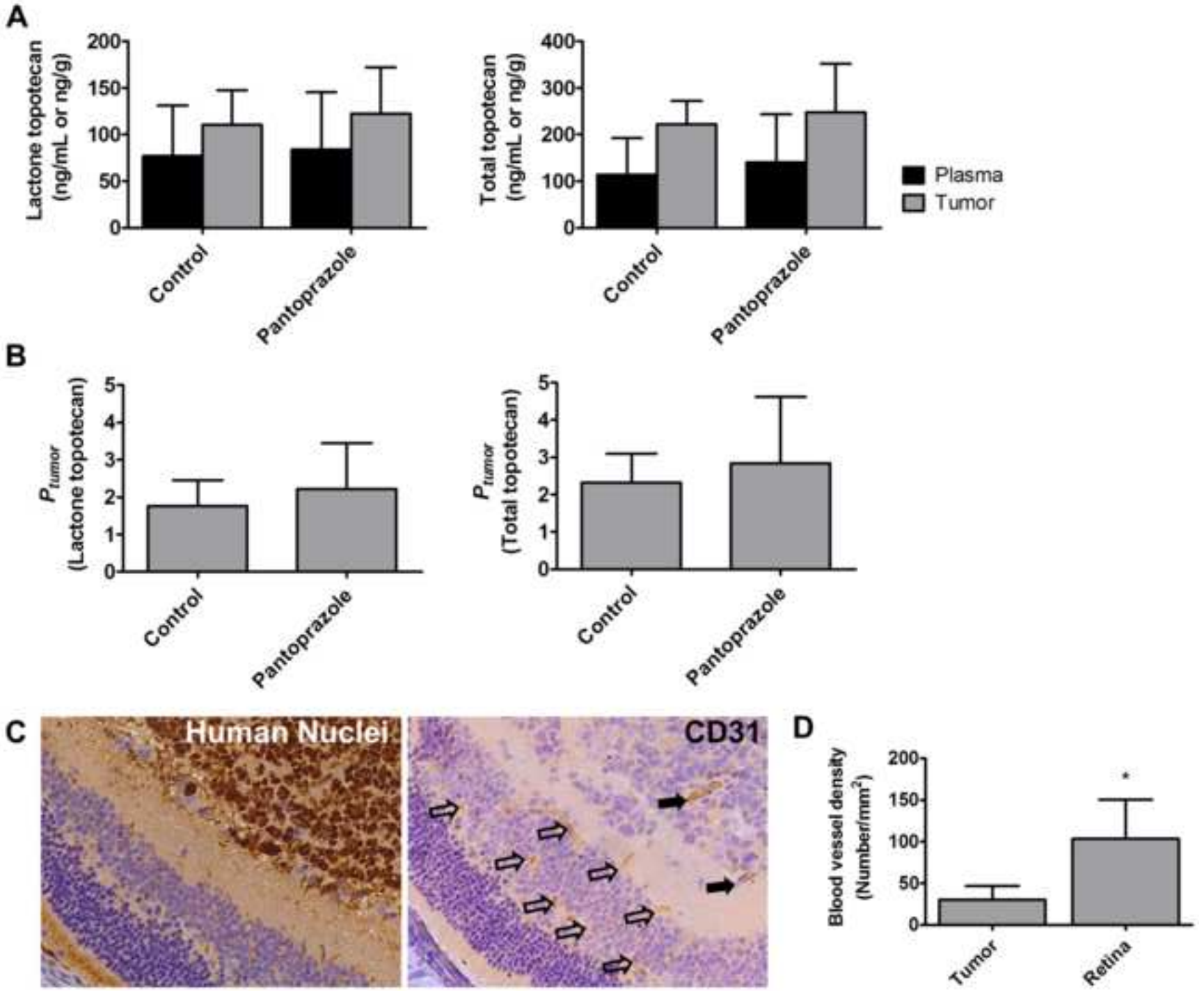

Figure(s)

Click here to download high resolution image

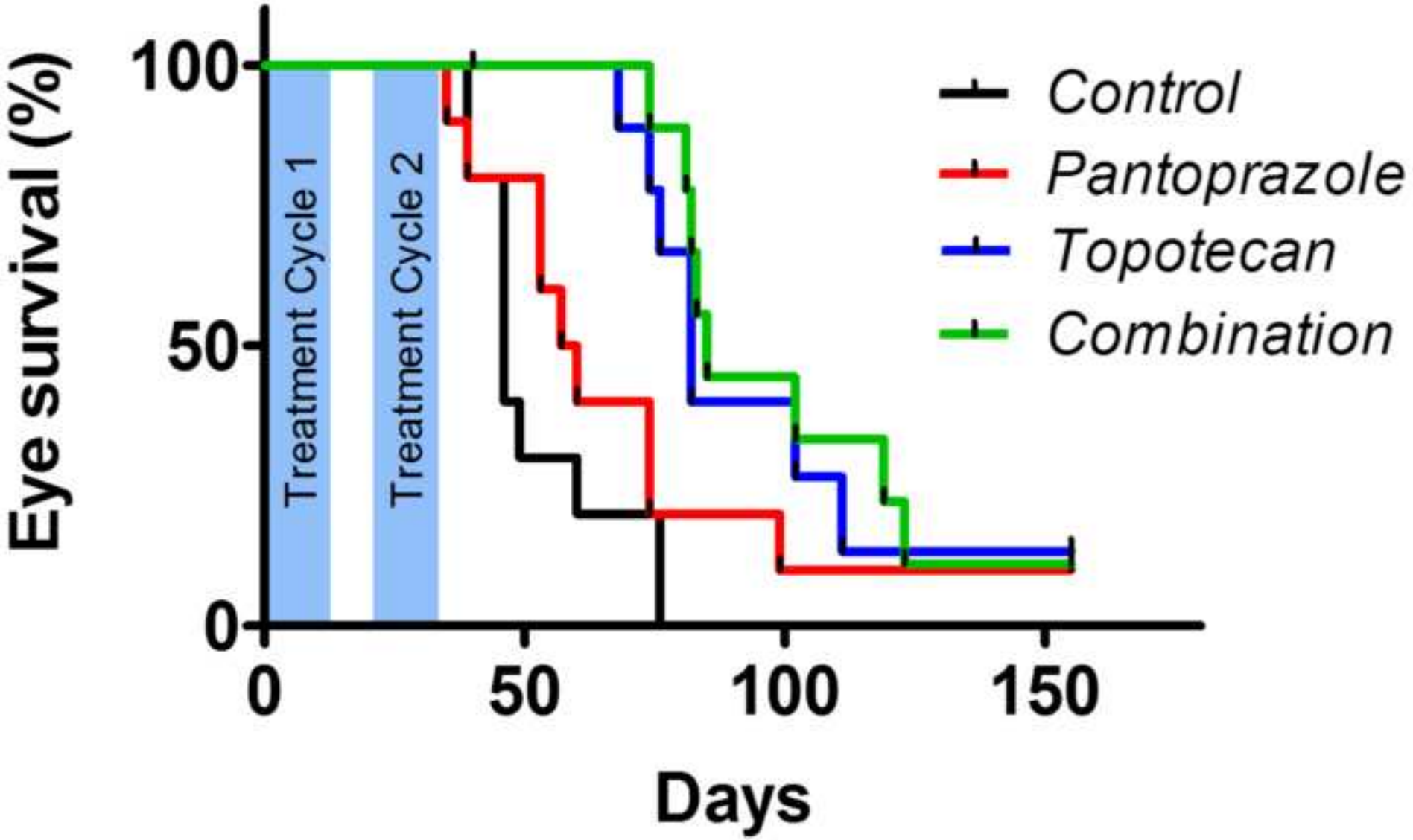

Figure(s)

Click here to download high resolution image

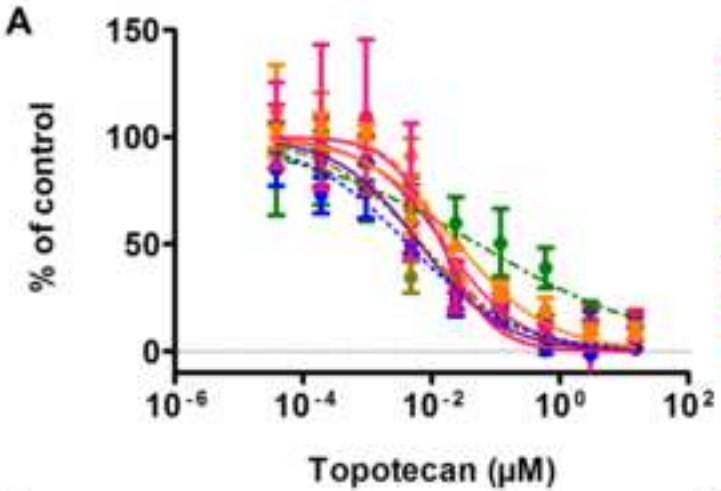

Retinoblastoma	Topotecan IC50 (nM) (95% Confidence Interval)
HSJD-RBT-1	15.9 (11.5-21.9)
HSJD-RBVS-1	4.39 (2.94-6.56)
HSJD-RBT-2	17.3 (12.0-25.1)
HSJD-RBVS-3	7.12 (4.6-10.9)
HSJD-RBT-5	53.1 (28.1-100.3)
HSJD-RBT-7	6.63 (4.81-9.14)
HSJD-RBT-8	14.5 (8.45-25.0)
Y79	25.9 (19.3-34.9)

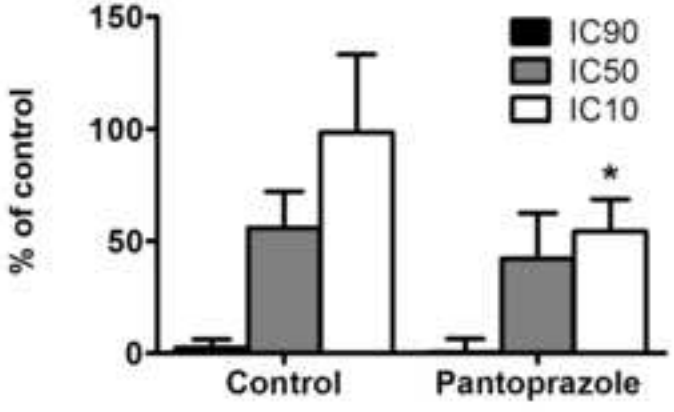

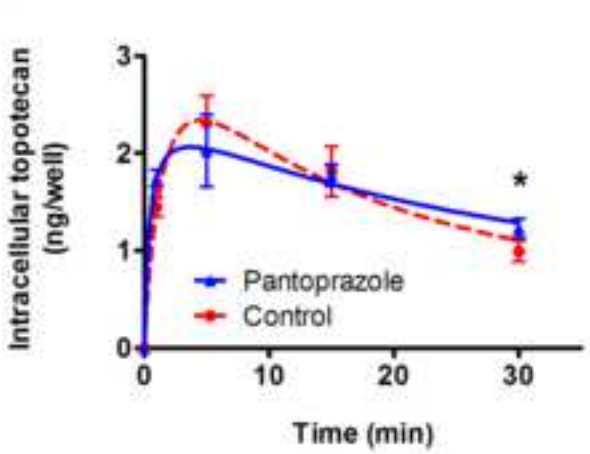

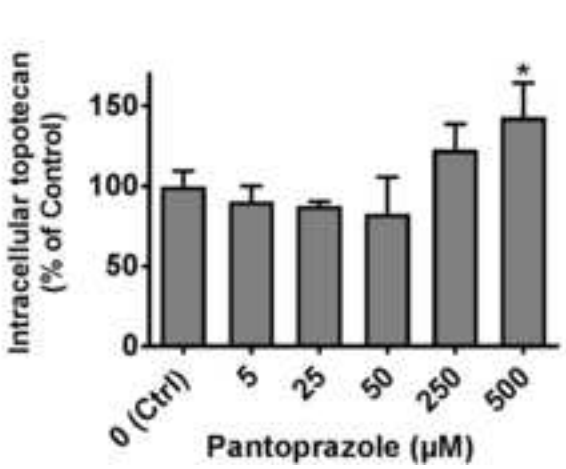

Supplementary Material

Click here to download Supplementary Material: Pascual-Pasto Supplemental Material v23.pdf